JOURNAL OF SPACECRAFT AND ROCKETS
Vol. 47, No. 3, May–June 2010

Interim Access to the International Space Station Using Evolved Expendable Launch Vehicles

Stephen A. Whitmore* and Tyson K. Smith†
Utah State University, Logan, Utah 84322

DOI: 10.2514/1.46750

This paper explores mission scenarios using existing evolved expendable launch vehicles for delivering, on an interim basis, the crew exploration vehicle Orion to the International Space Station. The use of existing commercial launchers is proposed to narrow the International Space Station service gap from the time the space shuttle is deserviced until the new Ares I launch vehicle is crew rated and operational. Here, three launch options are evaluated: 1) the Atlas V heavy-lift vehicle, 2) the Delta IV heavy-lift vehicle, and 3) the Delta IV with three common-core boosters (as a first stage, with the Orion acting as the second stage). Configurations 1 and 3 require significant impulse from the Orion's service-module engine to achieve the final orbit. Configuration 2 launches the Orion as a passive payload, without reliance on any impulse from the service module. All three configurations reserve sufficient service-module impulse for deorbit and reentry. Detailed simulation results, concepts of operation, and mission timelines are presented for each configuration. Mission feasibility is demonstrated for all three configurations. The final configuration has the advantage of eliminating failure paths and requiring human rating only for the common-core booster on the Delta IV system. Finally, reliability- and development-cost assessments are presented and compared with the Ares I.

Nomenclature

A_{exit}	=	nozzle exit area, m^2
C_D	=	drag coefficient
C_L	=	lift coefficient
e_{final}	=	final-orbit eccentricity, km
F_{drag}	=	aerodynamic drag force, kN
F_{lift}	=	aerodynamic lift force, kN
$F_{\text{thrust}}(t)$	=	engine thrust, kN
g_0	=	acceleration of gravity at sea level, 9.8067 m/s^2
I	=	orbital inclination, deg
I_{sp}	=	specific impulse, s
i_i	=	out-of-plane simulation coordinate
i_r	=	radial (vertical) simulation coordinate
i_v	=	longitudinal (horizontal) simulation coordinate
J_2	=	second gravitational harmonic
j	=	optimization iteration index
LH_2	=	liquid hydrogen
M_{dry}	=	dry spacecraft mass, kg
M_{prop}	=	propellant mass consumed during impulsive rocket burn, kg
$M_{\text{stage}(t)}$	=	current stage mass, kg
M_0	=	initial stage mass, kg
$\dot{m}$	=	engine mass flow, kg/s
n	=	pitch-profile decay exponent
P_{exit}	=	nozzle exit pressure, kPa
P_∞	=	ambient operating pressure, kPa
R_a	=	current-iteration final-orbit-apogee-radius, km
R_{target}	=	target orbit radius, km
r	=	radial distance from center of Earth, km
$T_{(t)}$	=	throttle
t	=	time, s
U_{exit}	=	nozzle exit velocity, m/s
V_r	=	radial (vertical) velocity, km/s
V_v	=	longitudinal (horizontal) velocity, km/s
Z	=	mean orbital altitude, km
Z_{final}	=	final-orbit mean altitude, km
α	=	angle of attack, deg
ΔV	=	velocity or effective energy change, km/s
γ	=	flight-path angle, deg
η	=	nozzle-exit angle, deg
$\theta(t)$	=	optimal pitch profile, deg
$\theta(t)_{\text{ballistic}}$	=	ballistic pitch profile, deg
ϑ	=	nozzle-exit correction factor
λ	=	pitch-profile decay slope parameter, $1/s^n$
ν	=	true anomaly angle, deg

Presented as Paper 6807 at the AIAA Space 2009 Conference and Exposition, Pasadena, CA, 14–17 September 2009; received 16 August 2009; revision received 12 January 2010; accepted for publication 13 January 2010.

*Assistant Professor, Mechanical and Aerospace Engineering Department, 4130 Old Main Hill, University Mail Code 4130. Associate Fellow AIAA.

†Graduate Research Assistant, Mechanical and Aerospace Engineering Department, 4130 Old Main Hill, University Mail Code 4130. Student Member AIAA.

I. Introduction

A NEW human-rated space transportation system is being developed by NASA's Constellation Program with the goal of establishing a sustainable human base on the moon. Key components of this system are the crew exploration vehicle (CEV), the lunar-surface-and-ascent module (LSAM), and the launch vehicles Ares I and Ares V [1]. The CEV crew module (CM) and service module (SM) configurations, collectively, are named Orion. The LSAM is named Altair. When development is complete, this system will become the primary human space-access system for the U.S., replacing all functions of the space shuttle. For missions to the moon, the proposed heavy-lift Ares V cargo-launch vehicle will launch the Altair lunar module and the Earth-departure stage (EDS). The Ares V launch will be followed by the Ares I launch, which will place the Orion spacecraft and crew into a low-Earth rendezvous orbit. The Ares I will launch the Orion to low-Earth orbit (LEO), where the crewed spacecraft will rendezvous with the LSAM, and the EDS will boost both vehicles into a translunar trajectory. The Ares I/Orion combination will also to be used to deliver the crew to the International Space Station (ISS). The Orion CM is patterned after the Apollo capsule, but it is significantly larger, with a diameter of 5.0 m (16.4 ft). A launch abort system (LAS) is designed to pull the crew and spacecraft to safety in the event of an emergency on the launch pad or a first-stage booster malfunction during ascent.

Ares I Ares V

Fig. 1 Ares launch vehicles.

Figure 1 shows the proposed Ares I and Ares IV configurations. The Ares I launch vehicle [2] is made up of an inline two-stage configuration, topped by the Orion spacecraft. The Ares I's first stage is based on a five-segment version of the reusable solid rocket motors (RSRM) used on the space shuttle. The first stage is mated to the upper stage via a newly designed forward adapter equipped with small solid motors that will separate the two stages during ascent. The upper stage features an upgraded and modernized version of the J-2 rocket engine that was previously used to power the Saturn IB and Saturn V upper stages. The upgraded version is referred to as the J-2X. Including the LAS, Ares I stands at 98 m (321 ft) tall when compared with the space shuttle, which is 56 m (184 ft) tall.

The heavy-lift Ares V configuration [3] will not be crew rated, and it is primarily designed for NASA lunar missions, but it may also be used for missions beyond the Earth–moon system. The vehicle is shuttle-derived, using two modified and five half-segment RSRM boosters and a core stage powered by five RS-68B engines for pad liftoff. The upper stage is the EDS, and it is powered by the J-2X rocket engine. The Altair landing vehicle is housed in the upper payload shroud. The Ares V stands at 116 m (381 ft). When built, the Ares V will be the largest and most powerful launch vehicle ever constructed.

With the space shuttle set to retire in early 2011, it is important that the Ares I become operational as soon as possible. During this interim period, NASA must rely on the Russian Soyuz or other possible Commercial Orbital Transportation Services (COTS) launchers for crew access to the station [4]. If the COTS options do not become operational, the U.S. will be at the mercy of foreign launch services for both crew transportation and servicing of the ISS [5]. Even if the currently proposed timeline is 100% successful, there will exist a 5 year operations gap for which the U.S. will not have self determined access to the ISS. Any further delay in the Ares I schedule will significantly impact, and could terminate, the ISS science and mission operations.

A preliminary structural analysis conducted on the Ares I indicated a potential first-stage longitudinal thrust oscillation (TO) that occurred near motor burnout [6]. These TOs are common problems in solid rocket motors [7], and they result when vortices shed during combustion resonate with the acoustic modes of the motor cavity. The predicted vibration levels exceed NASA's crew-health environmental specifications of 0.6 g rms (any axis) over a 1 min. duration during ascent [8]. Possible options that have been proposed to correct the oscillations include detuning the stack by modifying the propellant grain, active reaction control-system dampening, stiffening of the upper-stage structure, and adding isolation pads that would sit between the Orion and the J2-X stages.

The major programmatic risk lies in the lack of flight data for the five-segment booster flying in the Ares I configuration. To date, there exists only a ground-test-derived four-segment booster database and a small amount of data gathered by development flight instrumentation on the early STS-1 through the STS-4 and STS-9 flights. Because of this lack in flight data, and the immaturity of the Ares design, it is difficult to quantitatively assess the accuracy of the TO predictions and how the TOs will interact with the CEV systems and flight crew. All of these TO-mitigation design options are very immature, and they will undoubtedly take development and testing time. These design changes will inevitably reduce the Orion mass margins and will very likely delay the program schedule.

The first major demonstration test for the Ares I flight systems occurred on 10 September 2009 [9]. In this test, a five-segment development motor (DM-1) was static fired for approximately 2 min. to gather vibration and control data. The DM-1 motor tested the reformulated Ares I propellant and the modified throat and gimbal systems. Motor upgrades from a shuttle booster included the addition of a fifth segment, a larger nozzle throat, and an upgraded insulation and liner. The forward motor segment had also been improved for performance by adding another fin, or slot, in the upper propellant segment. This change in the geometry of the propellant provided additional surface area for burning the solid fuel, which resulted in greater thrust. The DM-1 nozzle throat was almost 8 cm wider in diameter than the nozzle used for the shuttle. The bigger nozzle throat allowed the motor to handle the additional thrust from the five-segment booster.

The second major demonstration, and first flight test, of the Ares flight systems occurred on 28 October 2009 [10]. The Ares I-X flight test was the first launch of the stand-alone RSRM and addressed configuration stability and control issues. The Ares 1-X trajectory closely approximated the planned Ares I launch profile, and it also included a pad avoidance maneuver (PAM) to mitigate risks associated with a potential for tower recontact during launch. The Ares 1-X test also provided valuable vibration and performance data during the ascent. The Ares I-X was similar in size and mass to the actual Ares I launch system, but it included a combination of dummy and actual spaceflight hardware. The Ares 1-X was powered by a conventional four-segment RSRM, modified to include an inert fifth segment to simulate the mass of the Ares I five-segment booster. Mock ups of the upper stage and the Orion CM/SM and LAS were used to simulate the integrated spacecraft systems.

The Ares 1-X reached an acceleration of nearly 3 g and a peak Mach number of 4.76. The maximum achieved altitude was approximately 46 km. The first stage separated from the upper-stage simulator and parachuted into the Atlantic Ocean, roughly 240 km downrange of the launch site. Because of the PAM performed by Ares I-X, shortly after liftoff, the launch pad received significantly more direct rocket exhaust than occurs during a normal space shuttle launch. The result was substantial damage to the fixed service structure (FSS) [11]. This damage was anticipated by NASA, and the FSS will be removed for future Ares 1 launches.

During descent, two of the three main parachutes deployed normally (partially inflating), whereas the third streamed (unopened). The streaming parachute is believed to have snagged one of the two partially inflated canopies, deflating it. According to NASA, partial parachute failures are not uncommon in space-shuttle solid rocket boosters (SRBs), from which the Ares I-X is derived. Eleven partial

parachute failures have occurred to date on space-shuttle SRBs, most recently on STS-128 [12].

The Ares I-X was originally intended to be part of a five-flight test program scheduled to take place between 2009 and 2011. These flights include tests of the LAS and a flight test of the full-up flight system. Testing of the LAS will be conducted beginning in 2010 and conclude in 2012. NASA plans to follow the LAS tests by the Ares I-Y test, which will use a five-segment Ares I booster and a live LAS. The I-Y launch is currently scheduled for 2012. Funding for the Ares I-Y flight test is currently not budgeted, and the ARES I-Y flight test is in jeopardy of being canceled by congress. The integrated testing of the launch vehicle and capsule is scheduled for 2014. The first live-crew testing is scheduled to take place in 2015, with operational flights to the ISS in 2016.

II. Review of Human Spaceflight: The Augustine Committee Report

On 22 October 2009, the Review of U.S. Human Spaceflight Plans Committee, chaired by former Lockheed–Martin Chief Executive Officer Norm Augustine, released their final report, detailing the results of their six-month study. This team was chartered by the Office of Science and Technology Policy, with the charter to review the feasibility of current U.S. human spaceflight plans and develop a go-forward plan that would insure a "vigorous and sustainable path to achieving its boldest aspirations in space" [13]. This study addresses the future of the shuttle, the ISS, the Constellation Program, and the overall future of the U.S. human space program. The final report details the changing development schedule for the Ares I, originally to be fully operational by 2012, but it is now officially delayed to 2015. The study concluded that, with the current state of the Ares I development, it was probable that the Ares I would become fully operational no earlier than 2017. This operational date is two years after the ISS was currently scheduled to be deorbited.

The Augustine Commission discussed the option of extending the life of the ISS to 2020 in order to support the Ares I, but their findings showed that this life extension would have serious fiscal impacts for both NASA and partner-ISS countries. To shorten the 7 year gap from when the shuttle is scheduled to retire to when the Ares I is to become operational, the Augustine Commission discussed the possibility of extending the life of the shuttle for an additional year. In both cases, life extensions consumed funds that were to be shifted to the Ares I development. The study concludes that, in order for the 2017 Ares I timeline to be achieved, NASA will need an additional $3 billion U.S. dollars per year added to the Ares I budget. Their recommendation was to scrap the Aero-1 LEO option and to emphasize heavy-lift vehicle (HLV) development for extra-LEO human missions.

The Augustine Commission discussed the option of having the Orion capsule lifted to a LEO, using current evolved expendable launch vehicles (EELVs). In this discussion, they stated that adapting the current EELVs to the Orion capsule would introduce additional costs and schedule impacts. However, their final report suggested that these impacts would be significantly less than the cost and schedule required to develop the Ares I to operational readiness. The Augustine Commission clearly offered that using commercial launch vehicles for the future of U.S. human space presented a viable option.

III. Interim Access to the International Space Station

The space shuttle and Soyuz are currently the only available means for crew access to the ISS. Once the space shuttle is decommissioned in 2011, only the Soyuz will be available as a crew access option. Thus, as mentioned previously, until the Ares I becomes operational, the U.S. will be dependent on Russia for crewed access to the ISS. This study proposes to explore alternate EELV options for testing and deploying the Orion spacecraft. The proposed EELV options are offered as an interim solution until the Ares launch systems become operational. As such, the EELV options will provide a risk mitigation path. If fruitful, these alternate launch options would allow the operational gap for ISS Missions to be reduced by several years or, if Ares I development issues became large, to be reduced by as much as a decade. This study does not address the Ares I deployment schedule and fiscal feasibility; it simply offers the EELVs as a nearer-term option for providing human spaceflight access to the ISS. This option is especially attractive if the ISS life is extended to beyond 2020.

A. Historical Precedents

There is precedence for this risk mitigation approach. In 1997, the Naval Research Laboratory (NRL) was awarded a contract to construct a spaceworthy interim control module (ICM) [14] for the ISS. This module was intended to buy down risk in the case that the Russian ISS Zvezda SM was destroyed or not launched for an extended period of time. It was derived from a formerly classified Titan Launch Dispenser used to distribute reconnaissance satellites to different orbits. Although the ICM was never flown, it provided schedule insurance and political leverage for the U.S. The ICM is currently in caretaker status at the NRL's Payload Processing Facility in Washington, D.C.

B. International Space Station Overview

The ISS is an internationally developed research facility currently being assembled in LEO. Onorbit construction of the station began in 1998 and is scheduled to be complete by 2011. The station consists of a number of pressurized modules and unpressurized components that have been launched by space shuttle, Soyuz, and proton rockets The ISS is serviced by a wide variety of uncrewed vehicles, including the Russian Progress Vehicle, the European Space Agency's automated transfer vehicle, and the Japanese Space Agency's H-II Transfer Vehicle. The ISS has been continuously staffed since the first resident crew entered the station on 02 November 2000. The ISS has been visited by crews from 16 different countries.

The ISS lies at a high inclination and at an altitude that lies near the lower limits of what is normally considered to be LEO. The high inclination orbit was mandated when the U.S. teamed with the Russian Space Agency, and the 51.7 deg inclination was the lowest orbit that the Soyuz could reach from the Baikonur launch complex [15]. To allow a Soyuz rendezvous mission, the ISS orbit is maintained at altitudes varying from a minimum of 278 km (173 mile) to a maximum of 425 km (264 mile). At this orbit, the ISS constantly loses altitude because of atmospheric drag, and it needs to be boosted to a higher altitude several times each year. Orbit decay rates vary from day to day, and they are heavily influenced by thermospheric density changes due to solar activity. The low altitude of the ISS orbit requires continual reboost, using residual impulse margins available to both space shuttle and progress vehicles.

Figure 2 shows the changes in mean altitude Z experienced for a 12-month period, beginning 01 August 2008. The station-altitude reboosts are clearly visible, as is the significant decay that occurred during the long delay between shuttle missions during early 2009. As the sun enters a period of greater solar activity, and atmospheric drag becomes greater, [16], the mean altitude of the ISS will tend toward

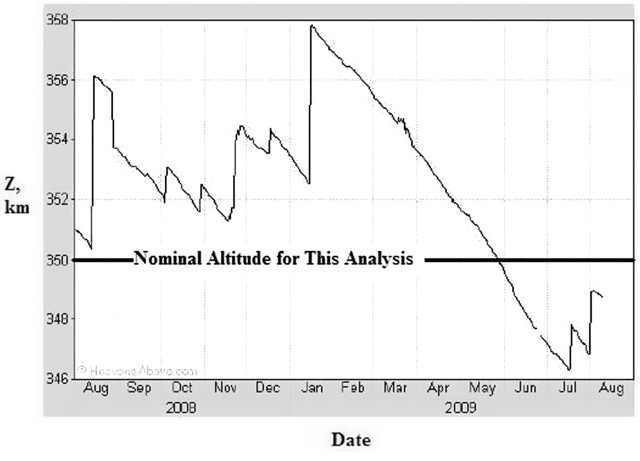

Fig. 2 ISS mean orbital altitude, August 2008–August 2009.

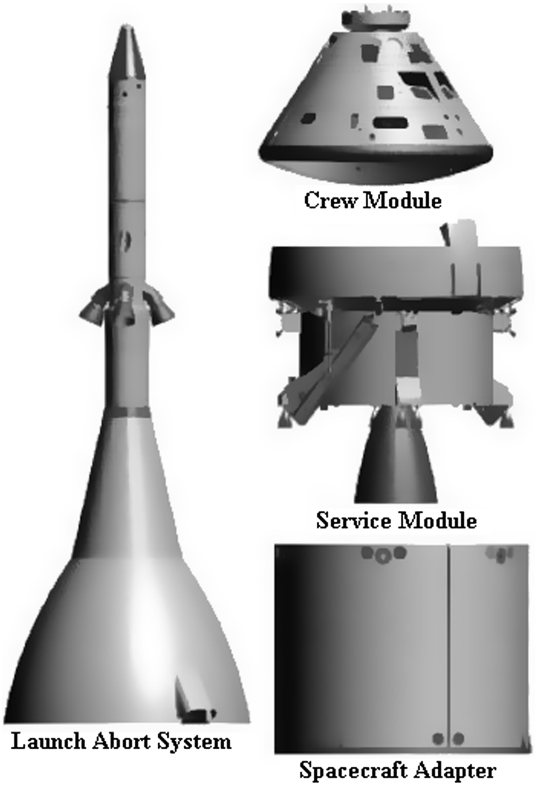

Fig. 3 Orion spacecraft components.

the lower ends of the nominal range. For the purposes of this study, the mean ISS altitude is defined to be 350 km above mean sea level.

IV. Preliminary Analysis of Available Launch Options

In keeping with earlier arguments considering near-term availability and U.S. launch determinism, only U.S.-licensed operational launch systems were considered for this study. Because of the high-orbit inclination, high LEO altitude, and large mass of the Orion spacecraft (to be described later), the only U.S.-licensed vehicles capable of performing the mission are the EELV platforms: Atlas V and Delta IV. The EELV configurations resulted from a program initiated by the U.S. Air Force after the Challenger accident in 1986. The EELV program [17] was intended to insure reliable access to space for the Department of Defense and other United States government payloads. Both systems use common components and feature a standard payload interface and a well-developed launch infrastructure. United Launch Alliance (ULA) currently operates both systems. In 2006, Holguin [18] performed a study addressing the issues associated with human rating the Atlas V launch system. Recently, Pulliam [19] performed a similar study for human rating the Delta IV heavy configuration. Both reports concluded that the tasks were feasible and affordable.

Table 1 CEV mass budget for ISS mission

Item	LAS	CM	SM	Launch adapter	Total
Dry mass, kg (lbf)	2596 (5722)	8779 (19,350)	4937.8 (10,883)	1639.7 (3614)	17,952.5 (39,567.3)
Propellant mass, kg (lbf)	4468.7 (9849)	136.1 (300)	3665.6 (8079)	——	8270.4 (18,228)
Consumable mass, kg (lbf)	——	35 (77)	206.9 (456)	——	241.9 (533.2)
Crew (4) mass, kg (lbf)	——	759.5 (1674)	——	——	759.5 (1674)
Gross launch mass, kg (lbf)	7064.7 (17,244.5)	9709.6 (19,726)	8810.3 (19,418)	1639.7 (3614)	27,224.4 (60,002.8)

Table 2 CEV mass budget for lunar mission

Item	LAS	CM	SM	Launch adapter	Total
Dry mass, kg (lbf)	2596 (5722)	8779 (19,350)	4115.7 (9071)	1639.7 (3614)	17,131 (37,756.7)
Propellant mass, kg (lbf)	4468.7 (9849)	136.1 (300)	7909.8 (17,433)	——	12,514.5 (27,582.2)
Consumable mass, kg (lbf)	——	35 (77)	314.9 (694)	——	349.9 (71.2)
Crew (4), lunar payload, kg (lbf)	——	859.3 (1894)	——	——	859.3 (1894)
Gross launch mass, kg (lbf)	7064.7 (17,244.5)	9809.5 (21,620.2)	12,340.4 (27,198.2)	1639.7 (3614)	30,854.5 (68003.0)

A. Proposed Orion Spacecraft Configurations

Table 1 itemizes the current mass budget for ISS configuration, and Table 2 itemizes the mass budget for the lunar mission. Excluding the LAS system, the ISS-mission mass to orbit for the CEV is 20,159.7 kg (44,432 lb), and the lunar-mission mass is 23,790 kg (52,433 lb). This value includes the mass of the spacecraft adapter, but it excludes the LAS mass. Including the LAS mass (jettisoned at stage 1 burnout), the ISS and lunar launch masses are 27,224.4 and 30.854.5 kg, respectively.

Figure 3 shows the CEV components as they sit atop the launch stack [20]. In the launch configurations to be studied, the Orion consists of four elements: 1) LAS, 2) CM, 3) SM, and the spacecraft/launch adapter. There are two versions of the design: a lunar-capable module and a module designed for ISS operations. The current crew size is four for both the lunar and ISS missions, with the primary mass differences being the additional propellant and consumables required for the longer-duration lunar mission. As listed in Table 2, the dry mass of the lunar version of the SM is smaller than the dry mass of the ISS version of the SM. Conversations with NASA have confirmed that these are the official numbers, as of the publication date of this paper.

B. Delta IV Launch Vehicle Family

Figure 4 depicts the Boeing Delta IV family of launch vehicles [21]. The Delta IV family [‡] is designed for optimum performance for a wide range of flight profiles. The Delta IV medium, medium-plus, and heavy configurations are evolved from the Delta II and III vehicles, and they combine highly reliable flight-proven systems [22]. As of 2008, ULA has successfully launched eight Delta IV vehicles. Delta IV's inaugural flight successfully launched Eutelsat's W5 commercial satellite on a medium-plus in November 2002 [23]. Two U.S. Air Force communication satellites were successfully launched on Delta IV medium vehicles in 2003, and the first heavy vehicle was launched in December 2004 [24].

The Delta IV design philosophy maximizes the use of common hardware. The Pratt and Whitney–Rocketdyne RS-68, liquid-hydrogen/liquid-oxygen (LOX/LH_2) engine powers the first stage. This engine is mounted to the common-core booster (CCB) first-stage structure, and it was designed for ease of manufacture by significantly reducing the part count, and thereby increasing reliability. The first-stage RS-68 engine can be throttled over a range from 60–100%. This feature is critical for human-crewed launches in order to reduce the maximum g loading. The Delta IV medium and medium-plus configurations use a single CCB augmented by either two or four 1.5 m GEM 60 solid strap-on rockets. The heavy-lift configuration replaces the strap-on solids by two strap-on CCBs. Each CCB is 5.1 m (16.7 ft) in diameter and 40.8 m (133.8 ft) long, and each uses 199,600 kg (440,000 lb) of propellants.

[‡]Data available online at http://www.astronautix.com/lvs/Atlas V.htm [retrieved 10 Aug. 2009].

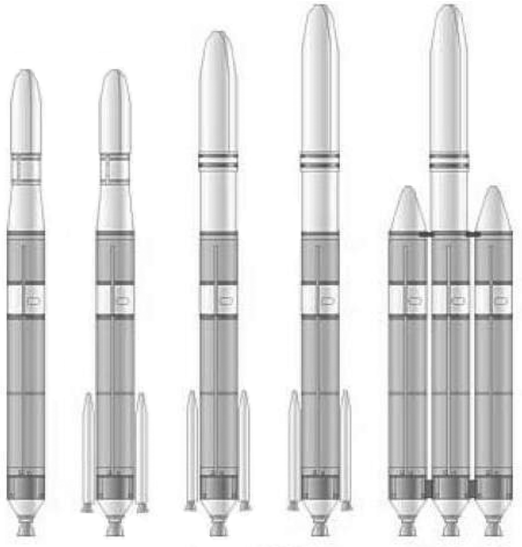

Fig. 4 Delta IV family of launch vehicles (M denotes medium and M+ denotes medium plus).

The cryogenic second stage is an evolutionary design incorporating the flight-control assembly from Delta II, and it is powered by the Pratt and Whitney–Rocketdyne RL10B-2 engine. The Delta II-derived upper-stage engine is capable of multiple restarts. The upper stage is 5.1 m (16.7 ft) in diameter and 12.1 m (40.0 ft) long, and it uses 27,200 kg (60,000 lb) of propellants. The payload fairing for the Delta IV medium and medium-plus configurations can use either a 4 m (13.12 ft) or 5 m (16.4 ft) fairing. The payload fairing for the heavy configuration is 5 m. The large size of the Delta IV heavy payload fairing is readily compatible with the 5 m diameter of the CEV spacecraft adapter.

Figure 5 ([21], page 103) shows the manufacturer's payload performance charts for the Delta IV medium-plus (Fig. 5a) and Delta IV heavy configurations (Fig. 5b). These charts plot the available payload as a function of the mean orbital altitude for three common inclinations available from the eastern launch range, complex SLC-37, at Cape Canaveral Air Force Station (CCAFS). Clearly, the Delta IV medium-plus configuration, even with four Graphite Epoxy Motors (GEM) 60 strap-on motors (5, 4 configuration), has insufficient payload capacity, approximately 13,400 kg (29,533 lb).

Alternatively, the Delta IV heavy payload capacity to a 51.6 deg inclination and 350 km circular orbit is approximately, 22,800 kg (50,251 lb). These graphs do not include the weight of the conventional 5 m payload fairing, approximately 3520 kg (7758 lb), or the upper-stage payload adapter, approximately 1500 kg ([21], page 119). For the CEV configuration, the mass of the Orion escape tower (7064.7 kg), jettisoned after stage 1 burnout, replaces the payload fairing mass. Similarly, the Orion spacecraft adapter mass (1639.7 kg) replaces the upper-stage adapter mass. When the 5 m fairing and upper-stage adapter masses are added to the payload mass from Fig. 5b, the lifted launch mass above the upper stage is 27,820 kg for the conventional Delta IV heavy configuration. This launch mass compares to 27,224.4 kg for the launch mass of the proposed ISS Orion configuration (Table 1).

Furthermore, it must be recognized that the payload masses presented in Fig. 5a are not optimized for a specific launch trajectory, and it is likely that the real launch vehicle will offer slightly higher payload capacities. Based on the discussion presented in the previous paragraph, it is concluded that the Delta IV heavy configuration has a sufficient launch margin to allow it to be carried forward as a viable launch option for the CEV.

C. Atlas V Launch Vehicle Family

Figure 6 depicts the Lockheed–Martin Atlas V family of launch vehicles [21] (see footnote [‡]). The Atlas V builds on features demonstrated on Atlas III and incorporates a structurally stable booster-propellant tank, enhanced payload fairing options, a common-core main booster, and optional strap-on SRBs. The CCB is 3.8 m (12.5 ft) in diameter, 32.5 m (106.6 ft) long, and uses 284,500 kg (627,100 lb) of LOX/RP-1 as propellants. The main CCB stage is powered by the Russian-built RD-180 engine. The first-stage RD-180 engine can be throttled over a range from 40–100%. The medium-lift configuration can use up to five strap-on boosters. The HLV configuration replaces the strap-on solids by two strap-on CCBs.

The upper Centaur III stage is powered by either one or two (optional) LOX/LH_2-propelled Pratt and Whitney–Rocketdyne RL10A-4-2 engine(s). The EELV's RL10A-4-2 engine features operational and reliability upgrades, compared with earlier versions of the design. The Centaur III stage is 3.1 m (10 ft) in diameter, 11.68 m (38.5 ft) long, and uses 20,830 kg (45,920 lb) of propellants. The nominal payload shroud is 4.1 m (13.45 ft) in diameter; however, an optional extended 5.4 m (17.7 ft) by 26.4 m (86.6 ft) payload fairing is available for the 500 series and HLV. The extended shroud weighs 5088 kg (11,214 lb).

The first four Atlas V (21 August 2002, 13 May 2003, 17 July 2003, and 17 December 2004) were successfully launched. On 14 April 2008, an Atlas V medium-plus configuration lifted its heaviest payload to date into orbit, a 14,625 lb (6,634 kg) telecommunications satellite built by Space Systems/Loral [25]. Although the HLV has never flown operationally, it is available for launch 30

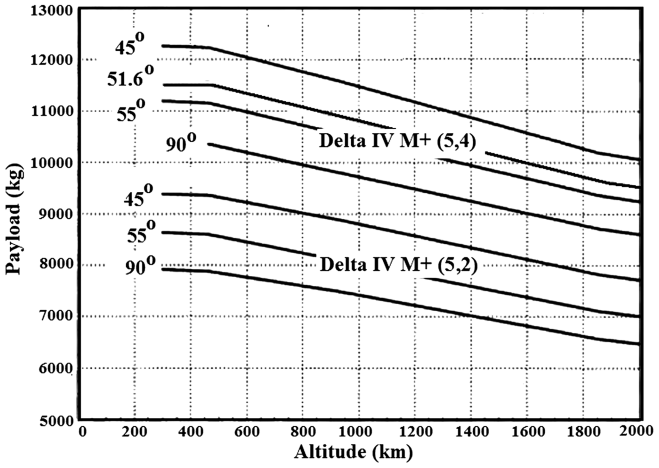

a) Delta IV M+, (5,2), (5,4) configurations

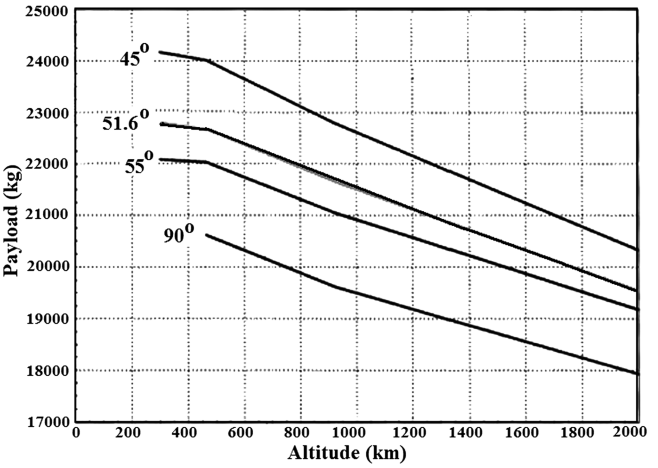

b) Delta IV Heavy configuration

Fig. 5 Delta IV medium-plus and heavy payload performance charts for LEO medium-Earth-orbit altitudes.

Fig. 6 Atlas V family of launch vehicles.

months from order [26]. The first operational flight of the HLV configuration is anticipated to occur in the 2012–2013 time frame.

Figure 7 shows the manufacturer's payload performance charts [27] for the Atlas V 552 medium and HLV configurations. Figure 7a plots the V-552 configuration's available payload as a function of the mean orbital altitude for three inclinations available from the eastern launch range, complex SLC-41, at CCAFS. Clearly, the 552 configuration has insufficient payload capacity, 17,600 kg (38,800 lb), to lift the required ISS Orion mass of 20,159.7 kg. Currently, payload charts for the V-HLV configuration are not available for public release; however, Fig. 7b shows the proposed baseline capability for the Atlas V configurations, and the stated low inclination lift capacity exceeds 27,000 kg for a 185 km altitude orbit [28].

As with the Delta IV preliminary analysis, these charts do not account for the launch tower, and the mass of the extended 5 m shroud [5088 kg (11,214 lb)], budgeted in these graphs, will not be carried during launch. This mass savings partially offsets the LAS mass and will be explored in detail in the Modeling and Simulation section. All things considered, the data presented in Fig. 7b are sufficiently positive to allow the Atlas V HLV to be carried forward as a viable launch option for the CEV.

V. Modeling and Analysis

This section takes the heavy-lift configurations described in the previous section and develops simulation models that allow the ISS–CEV-specific launch mission to be analyzed in detail and optimized. For this analysis, an interactive computer simulation developed at Utah State University (USU) was employed. The direct simulation offers the opportunity to optimize the mission-specific endoatmospheric portion of the launch trajectory, as well as allowing mission timelines to be constructed. This quasi-four-degree-of-freedom (DOF) simulation contains a graphical user interface (GUI) that allows direct in-the-loop control. The GUI also includes user-adaptable real-time displays.

The interactive simulation was used as a time-saving measure in lieu of more traditional trajectory-optimization tools, like the program to optimize simulated trajectories (POST) [29]. Some of the major drawbacks of POST are the labor of setting up the program for each configuration to be analyzed, time-intensive postprocessing, and sensitivity of the final solution to the initial trajectory guess. The USU interactive simulation allows the user to evaluate a wide array of possible maneuvers and trajectories in a very short period of time. The pilot-in-the-loop interactive simulation technique was pioneered at NASA in the 1960s and 1970s during the lifting body and follow-on flight-test programs [30]. This interactive simulation approach was paramount to this analysis, and it played a large role in allowing successful results to rapidly be achieved. The interactive USU simulation also allows perturbed conditions about the optimal trajectory for the Monte Carlo analysis [31] of orbit insertion inaccuracies.

A. Simulation Mechanics

The 3-DOF equations of motion are written as a six-state system of equations. The differential equations used to describe the vehicle dynamics are expressed in the satellite coordinate system and are integrated as an initial value problem with respect to time [32]. In this coordinate system, the i_r component points away from the center of the Earth in a radial direction and represents the local vertical for the spacecraft, the i_v component is perpendicular to the radial direction and represents in the local horizontal direction, and the i_i component is orthogonal to the other two axes and completes the right-handed coordinate system. This coordinate system stays fixed to the spacecraft at all times, and the i_i coordinate is always perpendicular to the instantaneous orbital plane. The angle of motion relative to the local horizontal is described by the flight-path angle γ. The direction of motion along the orbital track, relative to the Earth's equator, has an inclination angle I. The position of the spacecraft, relative to the orbital perigee, is described by the true anomaly angle ν, and the radial position of the spacecraft, relative to the center of the Earth, is designated by the symbol r.

At each data frame, the state-vector elements are transformed from the satellite reference frame to the Earth-fixed WGS-84 coordinate

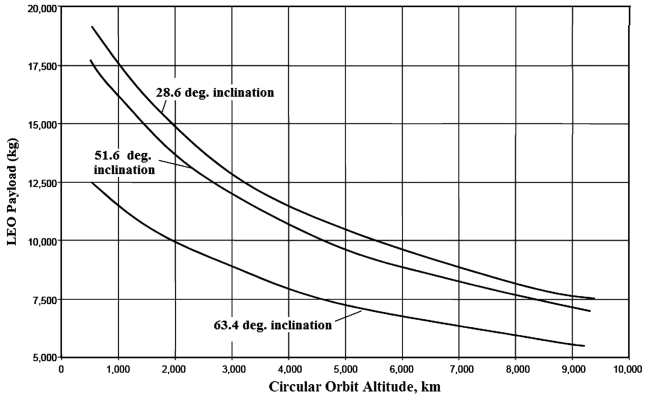

a) Atlas V, 552 medium

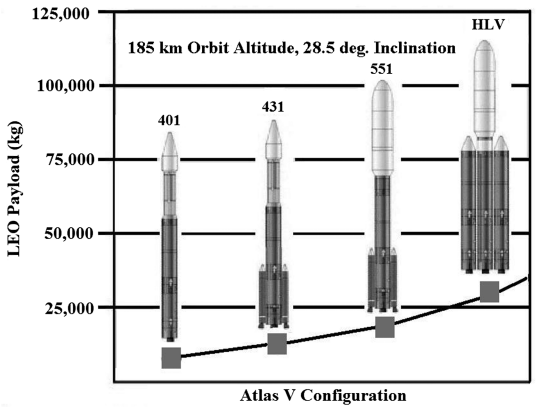

b) Proposed LEO capacity

Fig. 7 Atlas V payload performance charts for LEO medium-altitude orbits.

system. This transformation calculates the instantaneous orbital altitude, geodetic latitude, geocentric longitude, atmospheric properties, Mach number, dynamic pressure, angle of attack, and gravity vector direction. The oblate Earth model accounts for gravity out to the J_2 gravitational harmonic [33]. A constant Earth rotation rate is assumed. The atmospheric model can be selected to use either the 1976 United States Standard Atmosphere [34] or the 2007 Earth Global Reference Atmospheric Model (GRAM-2007) [35]. The spacecraft altitude is approximated as the difference between the spacecraft radius vector and the Earth radius at the local geodetic latitude.

The simulation is described as quasi 4-DOF, because the vehicle pitch angle can be prescribed independently of the equations of state. In this simulation, the pitch angle is defined as the angle between the vehicle longitudinal axis and the instantaneous horizontal plane. Pitch angle is designated by the symbol θ. The pitch angle can be controlled by preset waypoints, by a pitch-profile optimizer, or externally by inputs from a user-controlled video-game joystick. Increments to the prescribed nominal pitch angle can also be modified in real time by a pilot using the joystick input with user-selectable input gains. The pitch-profile optimizer will be described in more detail later in this section. As mentioned earlier, user-adaptable displays are available to the pilot and serve as aids for flying the desired trajectories.

Aerodynamic lift and drag forces act perpendicular to and along the direction of vehicle motion. The aerodynamic forces F_{lift} and F_{drag} are calculated from a table lookup of the trim lift and drag coefficients, expressed as a function of the angle of attack and Mach number. Hold-last values are used when the angles of attack in the lookup tables that were trimmed are exceeded. The methods used to calculate these aerodynamic force coefficients will be described in detail later in this section. The aerodynamic angle of attack is approximated as the difference between the pitch angle and the local flight-path angle, $\alpha = \theta - \gamma$. The vehicle is assumed to be trimmed at the prescribed angles of attack; inner loop stability is not accounted for in this simulation.

Thrust models were developed for each of the stage components. The features of these thrust models will be described in detail in the next section. The simulation throttle can be externally commanded by the user, using a joystick lever with user-selectable gains. This feature was used to limit the g loading that occurred during launch profiles. Interstage times between stage burnout and ignition and zero-g cost phases for the trajectory were simulated by setting the throttle to zero. Once proper throttle settings were determined interactively, the throttle settings were prescribed a priori, for each configuration and input to the simulation, using GUI front-panel inputs.

B. Evolved-Expendable-Launch-Vehicle Propulsive Stage Models

For these simulations, the mass-flow nozzle-exit velocity and nozzle-exit pressure were modeled using the one-dimensional De Laval flow equations [36] to allow thrust to be calculated as a function of the instantaneous local altitude. As mentioned earlier, these data were gathered from a variety of public domain sources and cross referenced for accuracy. Primary reference sources included [21], Encyclopedia Astronautica,[§] and Boeing and Lockheed–Martin web sites. The derived propulsion models account for the effects of changing ambient pressure and exit-cone angle momentum losses [37], and they allow for mass-flow-based engine throttling. The engine and stage properties, as modeled in the simulation for the Delta IV heavy, are presented in Table 3. Table 4 presents the engine and stage properties for the Atlas V HLV configuration.

The equilibrium gas-chemistry code chemical equilibrium with applications (CEA) [38] was used to model the combustion products based on mean properties for the specified propellants. The CEA code was developed at NASA Glenn Research Center, and it has been successfully applied for the analysis of rocket combustion, detonation, and flow across nonadiabatic shock waves. The code posits chemical reactions across the shock wave and then minimizes the Gibbs free energy [39] in order to reach thermodynamic and transport properties at chemical equilibrium. The CEA code has extensive internal libraries for gas thermodynamic and transport properties, including standard and nonstandard temperature and pressure conditions. The CEA-derived thermochemical data were adjusted as required to give consistency between the specified engine performance parameters and the one-dimensional thrust models.

C. Orion Propulsion Model

The Orion spacecraft's main propulsion system employs a single Aerojet AJ-10 rocket engine, derived from the second stage of the Delta II rocket.[¶] The engine uses nitrogen tetraoxide (N_2O_4) and monomethyl hydrazine (MMH) as propellants. These hypergolic propellants, although producing only mediocre performance, were selected as a safety feature. The design allows start and restart capabilities with only a simple injection system. The engine produces 33 kN (7,500 lb) of vacuum thrust. The primary SM engine use for LEO missions will be to maneuver Orion to the ISS and for deorbit and reentry. For lunar missions, the SM rocket engine will be fired to correct the translunar trajectory and to leave lunar orbit for the return trip to Earth. Table 5 presents the engine and stage properties for the Orion SM. Some of these data have been presented previously in Tables 1 and 2. The fully loaded ISS version of the CM/SM provides approximately 690 m/s (2270 ft/s) on onorbit maneuvering ΔV. The lunar version provides approximately 1400 m/s (4590 ft/s).

D. Throttled Propulsion Model Equations

Using the mass-flow, exit-area, exit-pressure, and exit-velocity data derived and presented in Tables 3–5, the throttled thrust equation is

$$F_{\text{thrust}(t)} = T_{(t)} \cdot \vartheta \cdot (\dot{m} \cdot U_{\text{exit}}) + (P_{\text{exit}} - P_{\infty}) \cdot A_{\text{exit}} \tag{1}$$

In Eq. (1), $F_{\text{thrust}}(t)$ is the time-variable thrust of the engine, $T_{(t)}$ is the throttle (variable over the prescribed range for the engine), P_{exit} is the nozzle-exit pressure, P_{∞} is the ambient operating pressure, U_{exit} is the nozzle-exit velocity, and A_{exit} is the nozzle-exit area. The parameter ϑ accounts for the nozzle-exit flow angle and, if η is the nozzle-exit angle, the correction is given by

$$\vartheta = \left(\frac{1 + \cos[\eta]}{2}\right) \tag{2}$$

The throttled mass depletion equation is

$$M_{\text{stage}(t)} = M_0 - \int_t (T_{(t)} \cdot \dot{m})\ \mathrm{d}t \tag{3}$$

In Eqs. (1) and (3), $\dot{m}$ is the nominal full-throttle mass flow listed in the tables, M_0 is the initial gross stage mass, and $M_{\text{stage}(t)}$ is the current stage mass (depleted as a function of time). The throttle is operable from 0 to 1.0. As mentioned earlier, ambient pressure is calculated as a function of altitude, using the 1976 U.S. Standard Atmosphere or GRAM-2007 models. The throttling term is included in the model to insure that g levels do not exceed crew-safety standards during ascent.

E. Orion Deorbit ΔV and Propellant Reserve Requirements

As mentioned previously, two of the mission scenarios to be analyzed rely on propulsive impulse being provided by the Orion AJ-10 engine. Thus, before proceeding with the simulation analysis, it was first necessary to establish the propellant reserve required to deorbit the CEV for reentry after undocking from the ISS. This process assumes an initial circular orbit, a 120 km (400,000 ft)

[§]Data available online at http://www.astronautix.com [retrieved 1 March 2009].

[¶]Data available online at http://www.astronautix.com/craft/orion.htm [retrieved 20 March 2010].

Table 3 Delta IV heavy propulsion stage properties

Simulation element	Stage 1 (core plus two boosters)	Stage 2
Engine	RS-68 (Rocketdyne)	RL 10B-2 (Pratt and Whitney)
Number of engines in stage	3	1
Length, diameter, m	40.8, 5.1	12.1, 5.1
Structural mass, dry mass, kg	26,800 (each), 80,400 (total)	3510
Wet mass, kg	226,400 (each), 679,200 (total)	29155
Propellant mass, kg	199,660 (each), 598,800 (total)	25645
Propellant mass fraction	0.8816	0.880
Propellant, mixture ratio	LOX/LH_2, 6	LOX/LH_2, 5.65
Thrust (vac), kN	3315 (each), 9945 (each)	110.1
Thrust (sea level), kN	2890 (each), 8670 (total)	——
Exit area, m^2	4.194 (each), 12.583 (total)	4,5452
Expansion ratio	21.5	285
Throat area, m^2	0.1951 (each), 0.58251 (total)	0.0630
Combustor pressure, Mpa	9.72	3.21
Combustor temperature, K	3600	3210
*I*sp (vac), s	420	462.4
Nozzle-exit angle, deg*I*sp	29.807	0
Burn time, s	248	1056.2
Ratio of specific heats (CEA)	1.160	1.150
Molecular weight (CEA)	13,138	15.2955
Mass flow, kg/s	804.84 (each), 2414.53 (total)	24.28
Nozzle-exit Mach number	3.641	5.1273
Nozzle-exit pressure, kPa	51.456	0.7589
Nozzle-exit velocity, m/s	3850.65	4389.43
Nozzle-exit temperature, K	1747.19	1172.5

atmospheric interface, and an impulsive deorbit burn. The algorithm used to calculate the required deorbit ΔV is based on the classical analysis presented by Milstead [40]. Figure 8 plots the resulting ΔV as a function of the initial orbital altitude and the entry interface flight-path angle. For a deorbit from the assumed 350 km ISS altitude, with a reentry flight-path angle of -1.5 deg, the required ΔV is approximately 105 m/s (378 ft/s).

From data presented in Table 1, the onorbit dry combined weight of the Orion CM and SM is 14,854.4 kg (32,739.1 lb). This mass conservatively includes all of the onboard consumables, except for the main engine propellant. Based on a rocket equation analysis [41], the required deorbit propellant mass reserve is

$$M_{\text{prop}} = M_{\text{dry}}\left[e^{\frac{\Delta V}{g_0 \cdot I_{\text{sp}}}} - 1\right] = 14,854.4\ \text{kg} \cdot \left[e^{\frac{105\ \text{m/s}}{9.8067\ \text{m/s}^2 \cdot 319.97\ \text{s}}} - 1\right] = 505.48\ \text{kg} \tag{4}$$

This mass amount will be decremented from the available mass for all simulation runs and budgeted as dry spacecraft mass.

F. Launch Vehicle Aerodynamics

Traditionally, the lift and drag coefficients of commercially operational launch platforms are closely guarded secrets and are not readily available in the public domain. An exhaustive literature search found no aerodynamic coefficient data for the two EELV launch systems being considered for this study. Thus, for this analysis, it was necessary to generate those estimates independently to facilitate the simulation studies. The aerodynamic characteristics for each configuration are calculated using Missile DATCOM (MDC). MDC is a semiempirical analysis tool developed at the Air Force Research Laboratory [41]. This code is the de facto aerospace and defense industry standard for modeling rocket and missile aerodynamics, and it has been in continual development for over 20 years. DATCOM predictions are valid for both subsonic and supersonic conditions, and extensive studies have demonstrated that the predictions are accurate for a variety of configurations at a moderate angle of attack [42]. DATCOM has been traditionally supplied free of charge by the USAF to American defense

Table 4 Atlas V HLV propulsion stage properties

Simulation element	Stage 1 (core plus two boosters)	Stage 2
Engine	RD-180 [Research Production Org. (NPO) Energomash]	RL10A-4-2 (Pratt and Whitney)
Number of engines in stage	3	1
Length, diameter, m	32.5, 12.5	11.68, 3.05
Structural mass, dry mass, kg	18,800 (each), 56,400 (total)	2130
Wet mass, kg	276,500 (each), 829500 (total)	22,960
Propellant mass, kg	257,700 (each), 773,100 (total)	20,830
Propellant mass fraction	0.932	0.907
Propellant, mixture ratio	LOX/RP-1, 2.27	LOX/LH_2, 5.85
Thrust (vac), kN	4152 (each), 12,456 (total)	198.4
Thrust (sea level), kN	3827 (each), 11,481 (total)	——
Exit area, m^2	3.2085 (each), 9.6225 (total)	2.384
Expansion ratio	36.87	85
Throat area, m^2	0.0870 (each), 0.261 (total)	0.02805
Combustor pressure, Mpa	25.76	3.21
Combustor temperature, K	3020	3530
*I*sp (vac), s	337.8	450.5
Nozzle-exit angle, deg	28.8	0
Burn time, s	205.6	463.8
Ratio of specific heats (CEA)	1.1162	1.1449
Molecular weight (CEA)	24.24	16.32
Mass flow, kg/s	1253.3 (each), 3759.9 (total)	44.916
Exit Mach number	3.753	4.376
Exit pressure, kPa	82.557	3.33
Exit velocity, m/s	3101.7	4062.6
Exit temperature, K	1594.9	1479.5

Table 5 Orion propulsion module properties

Simulation element	Orion/SM data
Engine	AJ-10 (aerojet)
Number of engines in stage	1
Length, diameter, m	4.78, 5
Structural mass, dry mass, kg	5144.7 (ISS), 4430.6 (lunar)
Wet mass, kg	8810.3 (ISS), 12,340.4 (lunar)
Propellant mass, kg	3665.6 (ISS), 7909.8 (lunar)
Propellant mass fraction	0.426 (ISS), 0.641 (lunar)
Propellant, mixture ratio	N_2O_4/MMH, 1.7
Thrust (vac), kN	33.4
Exit area, m^2	0.6137
Expansion ratio	85
Throat area, m^2	0.00722
Combustor pressure, Mpa	2.5
Combustor temperature, K	3300
*I*sp (vac), s	319.97
Nozzle-exit angle, deg	0
Burn time, s	344.4
Ratio of specific heats (CEA)	1.278
Molecular weight (CEA)	21.891
Mass Flow, kg/s	1253.3 (each), 3759.9 (total)
Exit Mach number	5.424
Exit pressure, kPa	1.410
Exit velocity, m/s	3056.6
Exit temperature, K	654.3

contractors. The program is written in Fortran 90, and both compiled and source code versions are available. A detailed user's guide [43] is available. The DATCOM program is available commercially as a compact disk, included with Hammond's [44].

The MDC program calculates aerodynamic force and moments coefficients and nondimensional vehicle stability derivatives. Only the lift and drag coefficients were used in this analysis. All calculations by MDC are performed in the total angle-of-attack/aerodynamic-roll coordinate system, commonly known as the aeroballistic axis system [45]. MDC uses a component buildup superposition approach for calculating the forces and moments. With this technique, estimates are made for isolated body and fin panels. Semiempirical interference effects are then applied, and the results are summed to give the overall aerodynamic coefficient, moment, etc. Program inputs include Mach number, angle of attack, Reynolds number ranges, and the physical geometry of the body. Physical coordinates include nose, body, and fin characteristics. Optionally, flat-plate models, adjusted for compressibility, can be used to account for skin friction effects.

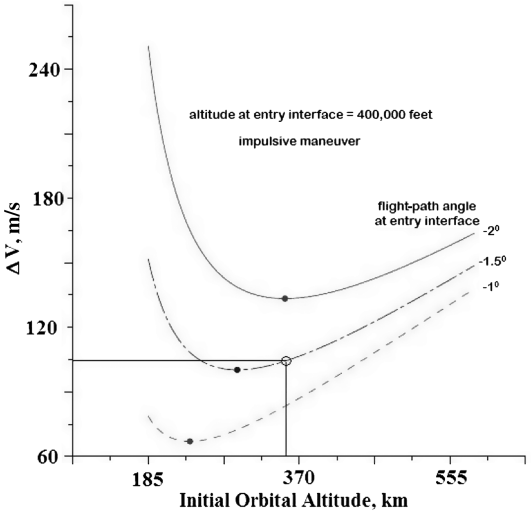

Fig. 8 ΔV required for Orion deorbit from ISS.

Figure 9 presents the MDC-derived aerodynamic data for the Delta IV heavy in launch configuration. Figure 9a plots the lift coefficient C_L as a function of the angle of attack and Mach number. The reference area for the Delta IV coefficients is 52.04 m^2. Figure 9b plots the drag coefficient C_D. Figure 10 presents similar lift and drag data for the Atlas V HLV. The reference area for the Atlas V coefficients is 34.05 m^2. Only the engine-on launch-configuration aerodynamics were accounted for. This analysis ignores the effects of atmospheric drag. As expected for both configurations, when the angle of attack rises beyond 10 deg, a severe drag penalty is encountered.

The data presented in Figs. 9 and 10 are rough estimates of the vehicle aerodynamics. Because this paper is intended to only demonstrate feasibility, no formal aerodynamic uncertainty analysis was performed. Based on data presented by Cobleigh [46], the estimated uncertainty of the drag coefficients is estimated at 15% of the value, and the lift uncertainties are estimated at 8% of the value. Although these uncertainty values can be considered large, the trajectory optimization has the effects of minimizing the aerodynamic penalty, and the aerodynamic uncertainties have minimal effect on the overall lift masses.

G. Pitch-Profile Optimization

As mentioned earlier, an endoatmospheric pitch-profile optimization routine is available as part of the USU simulation code. Once initial mission feasibility was established by interactively flying a notional pitch profile, this option was used to refine the final trajectory. During the endoatmospheric launch phase, an apogee-targeting strategy was used to deliver the payload (including any propellant and stages required for orbit circularization and trim) to a stage 2 burnout orbit with an apogee that was just below the desired final altitude and maximum energy level. The assumption here is that after the stage 2 burn, the vehicle is high enough that atmospheric effects are minimal. Exoatmospheric circularization and trim burns

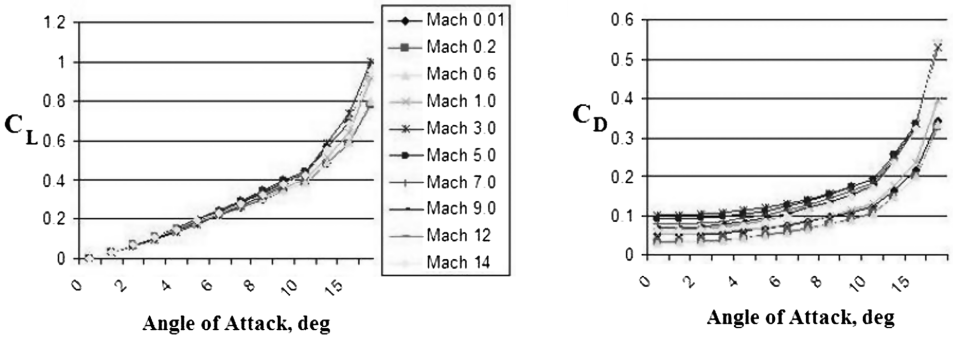

a) b)

Fig. 9 Delta IV heavy aerodynamic coefficients.

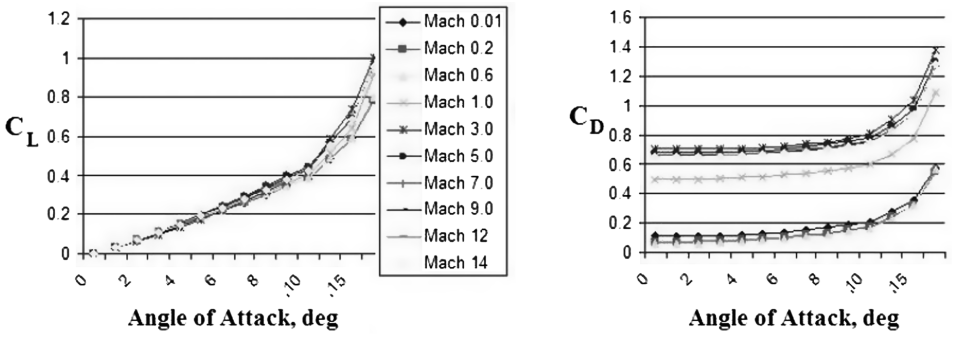

a) b)

Fig. 10 Atlas V HLV aerodynamic coefficients.

are most efficiently achieved at orbit apogee, with a burn angle directed along the direction of travel.

Even though the ballistic launch profile offers the minimum drag solution, it also produces a very lofted trajectory that reaches the ISS orbit altitude with minimal forward velocity. For a ballistic profile, there is insufficient centripetal acceleration to hold the vehicle at altitude, and gravity losses (thrust required to lift the vehicle) overwhelm any drag savings. Performing a gravity turn ([47], chapter 9) soon after the launch allows centripetal force to hold the vehicle at altitude, and thrust is used to achieve forward acceleration. The pitch profile is optimized, starting with the ballistic launch profile, and then systematically turns the corner during successive launch iterations. The optimal profile is modeled as an exponential decay or growth in time from the ballistic pitch profile, using a two-parameter model:

$$\theta(t) = \theta(t)_{\text{ballistic}} \cdot e^{-\lambda \cdot t^n} \approx \tan^{-1}(V_r/V_v) \cdot e^{-\lambda \cdot t^n} \tag{5}$$

In Eq. (2), $\theta(t)$ is the optimal pitch profile, $\theta(t)_{\text{ballistic}}$ is the ballistic profile, λ is a pitch decay slope parameter, n is a scaling exponent, and t is time from launch. The exponential decay produces a smooth turn and assures that angles of attack remain small during the endoatmospheric burn. This small angle of attack limits aerodynamic side loading on the launch stack, and it keeps the aerodynamic drag penalty at a minimum value. Because the local angles of attack are small, the ballistic pitch angle can be approximated by the inertial flight-path angle, where

$$\gamma = \tan^{-1}(V_r/V_v) \cdot e^{-\lambda \cdot t^n} \tag{6}$$

Parameter iterations are implemented as two loops, with n being iterated in the outer loop and λ driven to a value that satisfies the apogee constraint in the inner loop. In the optimization process, the parameters $\{\lambda, n\}$ are set at the beginning of the simulation run and fixed as a function of time for that run. The pitch-profile parameters are iterated between simulation runs to satisfy the apogee constraint and maximize orbital energy. The inner apogee constraint is satisfied, using a modified Newton–Raphson method [48]:

$$\lambda^{(j+1)} = \lambda^{(j)} - \left(\frac{R_a^{(j)} - R_{\text{target}}}{R_a^{(j)}}\right)\lambda^{(j)} \tag{7}$$

In Eq. (7), the parameter R_a is the orbit apogee at stage 2 burnout, R_{target} is the target orbit radius, and j is the current iteration index. Each inner-loop iteration represents a complete run of the endoatmospheric (stages 1 and 2) portion of the simulation.

Because the stage 2 burnout apogee is constrained, maximizing the vehicles orbital energy is equivalent to maximizing the stage 2 burnout perigee radius. The parameter pair that gives the largest stage 2 burnout perigee radius (orbital energy) and satisfies the apogee constraint provides the optimal pitch profile. This ad hoc optimization method is used in lieu of the more traditional Lagrange multiplier ([32], chapter 7) methods to save calculations, speed convergence, and allow the existing interactive simulation code to be used entirely without modification. Whitmore and Smith [49] derived this method and described its use in detail. The local vertical velocity V_r and horizontal velocity V_v are produced by launch trajectory and are not independent parameters to be optimized.

VI. Results and Discussion

During preliminary studies, a whole suite of launch profiles and EELV configurations were modeled, including options for which the CEV/Orion was lifted to orbit as an inert payload, with the launch vehicle providing all of the required impulse, and options for which a fraction of the available ΔV from the Orion SM was used for final-orbit insertion and trim. The most promising three options, one for the Atlas V and two for the Delta IV, will be presented here. Each configuration reaches the ISS with sufficient propellant margin to allow for the deorbit burn described in the previous section. The following sections describe these configurations, develop mission timelines, and present detailed launch trajectories. Figure 11 shows these preferred configurations.

A. Atlas V Heavy-Lift-Vehicle Crew-Module/Service-Module Active Configuration

This section presents results for the first configuration of Fig. 11. This configuration uses the first and second stages of the Atlas V HLV, with the payload stage replaced by the CM/SM. The proposed configuration assumes that the Orion spacecraft adapter has been modified to interface with the Centaur III upper stage. For this configuration, both EELV stages are fully loaded with propellant and consumed to depletion during launch. The CM/SM is loaded with propellant for the ISS mission (3665.6 kg). A portion of the available CM/SM ΔV is required for final ISS orbit insertion and trim, thus the designator CM/SM active. Fig. 12 shows the proposed mission concept of operations (CONOPS). The table in Fig. 12 shows the mission timeline from launch to final-orbit insertion. This trajectory is intended only to demonstrate the mission feasibility. Mission timelines due to specific phasing orbits required to rendezvous with the ISS are not considered in this analysis.

Figure 13 presents the optimized trajectory, showing time-history profiles for altitude, pitch angle, acceleration, and velocity. The time axis is plotted on a logarithmic scale to enhance features early in the launch profile. This trajectory results from the optimized endoatmospheric pitch profile. Here, the target apogee at stage 2 burnout was 350 km, and the resulting optimized parameter pair is $\{\lambda = 0.0813\ \text{s}^{-0.54},\ n = 0.503\}$. Figure 13b also plots the minimum drag (ballistic) profile for this launch apogee. Clearly, the optimal profile differs dramatically. Here, the vehicle rises almost vertically for the first 10 s and then pitches over. At stage 1 burnout, the optimal pitch angle is down to 15 deg, compared with 35 deg for the ballistic trajectory. By turning the corner early in the launch, centripetal acceleration supports the vehicle weight, and the propulsive thrust is used to accelerate the vehicle.

The staging events are very apparent in the acceleration and velocity profiles. The launch events are labeled on the acceleration plot in Fig. 13c. The acceleration plot also overlays the commanded throttle for the vehicle. At approximately 140 s, the first-stage engines are throttled back linearly with time from 100 to 53% to insure that the crew-sensed acceleration does not exceed 7.0 g. This acceleration limit is an environmental constraint specified by NASA's crew-safety limits [50]. The vehicle is scheduled to throttle back when 4.0 g acceleration is reached. The throttling slope was

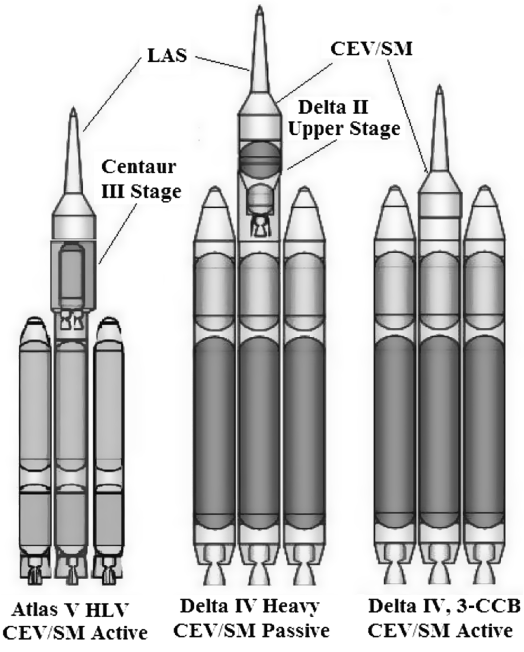

Fig. 11 Preferred EELV configurations for ISS Orion mission.

selected interactively to insure that the 7.0 g limit was not exceeded. The long Keplerian coast from the second-stage burnout to the CM/SM ignition is the time required to reach the orbit apogee at 350 km. During this period, the vehicle is in microgravity and is falling toward the orbit apogee. The final burn circularizes and trims the orbit. The final-orbit eccentricity for the optimal simulation run is 0.0004.

When the ISS orbit is reached, the CM/SM has approximately 840 kg of propellant remaining. Thus, approximately 77% of the available propellant for the CEV main engine was used. Because only slightly more than 500 kg of propellant are required for deorbit and reentry, there is more than sufficient reserve for the deorbit burn, and any onorbit maneuvering that may be required. Any residual propellant can also be used to reboost the ISS after docking. Unfortunately, this propellant reserve is insufficient to allow loss of a first-stage CCB engine and still have sufficient impulse to be able to achieve the ISS orbit.

No.	Event	Time, sec	Mean Altitude, km
1	Stage 1 Ignition/Liftoff	0	0
2	Stage 1 Burnout/ CCB Separation	228.45	67.25
3	LAS Tower Jettison	231.05	68.0
4	Stage 2 Ignition	233.45	95.90
5	Stage 2 Cutoff	574.05	69.7
6	CEV/SM Engine Ignition	1648.15	349.5
7	CEV/SM Engine Cutoff	1724.0	349.94
8	Orbit Insertion	1724.5	349.94

Fig. 12 Launch CONOPS: Atlas V HLV CM/SM active.

B. Delta IV Heavy-Configuration Crew-Module/Service-Module Passive Configuration

The second configuration shown in Fig. 11 uses the first and second stages of the Delta IV heavy, with the payload stage replaced by the CM/SM. The configuration assumes that the Orion spacecraft adapter has been modified to interface with the Delta II upper stage. For this configuration, both EELV stages are fully loaded with propellant and consumed to depletion during launch. The CM/SM is fully loaded with propellant for the ISS mission (3665.6 kg); however, none of the available CM/SM ΔV is used to reach the ISS orbit. Thus, this mission is designated as CM/SM passive.

The first and second stages provide sufficient impulse to achieve the desired final ISS orbit. The upper stage is burned twice, with the first burn used to reach the desired final-orbit apogee of 350 km altitude. Trajectory optimization is performed up to only the first stage 2 burn termination. The second burn is used to circularize and trim the final orbit at apogee. If the CM/SM ΔV is used, this configuration has sufficient reserve to allow loss of a first-stage engine and still achieve the ISS orbit. Managing the vehicle stability in the advent of a first-stage core-engine loss is beyond the scope of this analysis. Figure 14 shows the proposed mission CONOPS, and the table in Fig. 14 shows the mission timeline from launch to final-orbit insertion. As stated previously, this trajectory is intended only to demonstrate the mission feasibility; phasing orbits required to rendezvous the ISS are not considered in this analysis.

Figure 15 presents the optimized trajectory, showing time-history profiles for altitude, pitch angle, acceleration, and velocity. Here, the target apogee at stage 2 burnout was 350 km, and the resulting optimized parameter pair was $\{\lambda = 0.1096\ \mathrm{s}^{-0.54},\ n = 0.499\}$. For

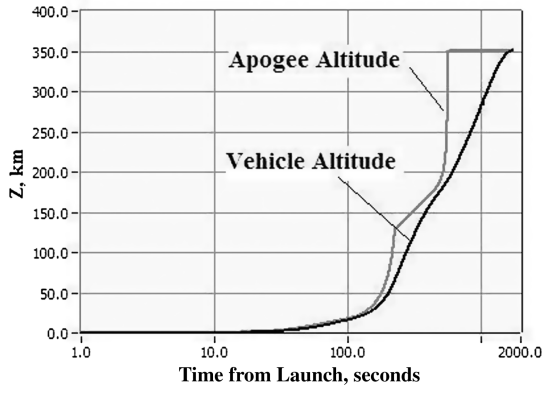

a) Geometric altitude/orbit apogee

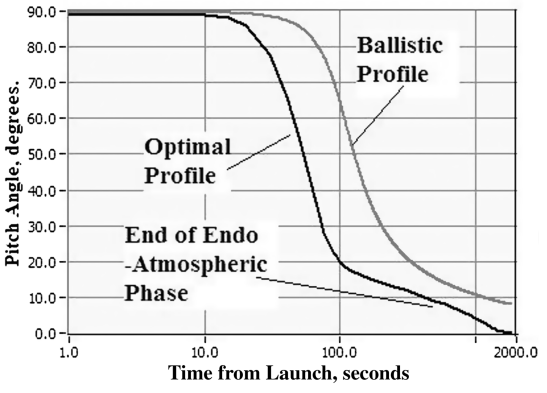

b) Pitch angle

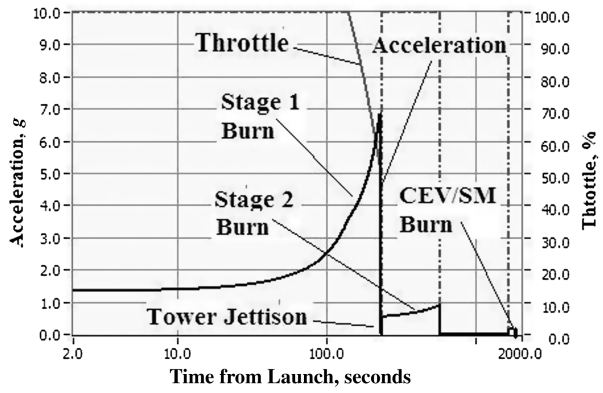

c) Onboard acceleration, throttle

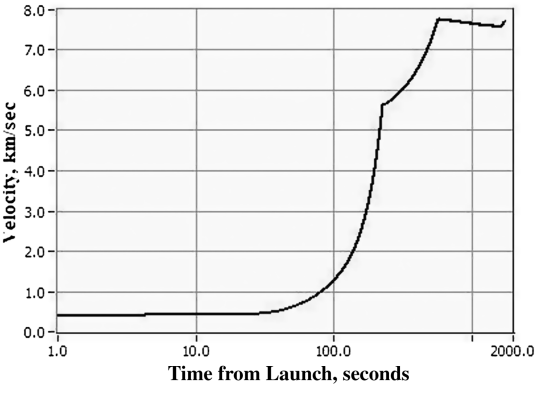

d) Inertial velocity

Fig. 13 Atlas IV HLV CM/SM active optimal trajectory.

the trajectory, the endoatmospheric optimization routine was terminated at the first stage 2 burn shutoff (984 s) and then manually faired to zero for the circularization and trim burn. Because of the large total impulse provided by the first-stage CCBs, this trajectory has a distinctly different look than the Atlas V trajectory presented in Fig. 13. Here, the optimized profile nearly reaches the final orbit during the second burn. When compared with the trajectory presented in Fig. 13, the Keplerian coast phase of this trajectory is very short. In the first burn of stage 2, 23,300 kg of propellant are consumed, approximately 90.5% of the available propellant. In the second burn, approximately 2060 kg of propellant are consumed for the circularization and trim burn, accounting for 98.5% of the total second-stage propellant. Because the CM/SM has been delivered with a full-ISS propellant load, there is considerable reserve propellant for onorbit operations, including reboost of the ISS. This option could prove valuable in the case that the Russian Progress or Soyuz spacecraft are no longer available for ISS station keeping and orbit maintenance.

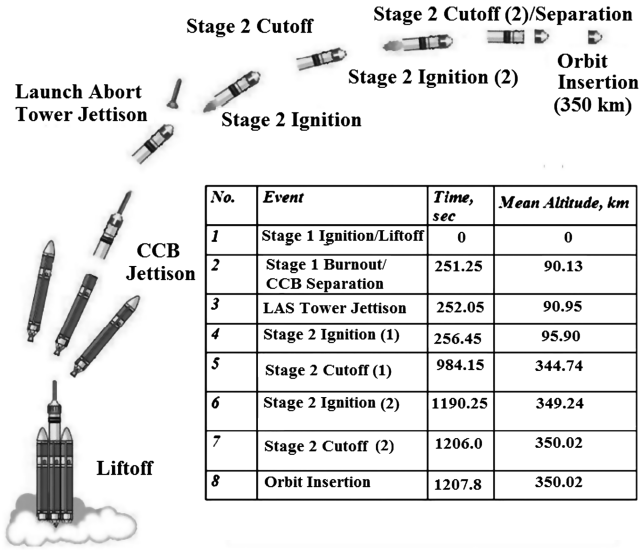

No.	Event	Time, sec	Mean Altitude, km
1	Stage 1 Ignition/Liftoff	0	0
2	Stage 1 Burnout/ CCB Separation	251.25	90.13
3	LAS Tower Jettison	252.05	90.95
4	Stage 2 Ignition (1)	256.45	95.90
5	Stage 2 Cutoff (1)	984.15	344.74
6	Stage 2 Ignition (2)	1190.25	349.24
7	Stage 2 Cutoff (2)	1206.0	350.02
8	Orbit Insertion	1207.8	350.02

Fig. 14 Delta IV heavy CM/SM passive CONOPS.

C. Delta IV Three-Common-Core-Booster Crew-Module/Service-Module Active Configuration

As demonstrated in the previous section, the Delta IV heavy configuration has significant excess capacity for the ISS mission and can lift the entire Orion configuration as a passive payload. This section examines the intriguing possibility that the ISS mission can be accomplished using only the first stage of the Delta IV heavy and the fully (lunar mission) loaded CM/SM. If feasible, this configuration has the distinct advantage of simplifying the launch stack, thereby reducing potential failure paths. The proposed configuration also eliminates the need to human rate the upper Delta II stage. Because only the CCB needs to be human rated for this configuration, there exists a tremendous potential for schedule compression and cost savings.

For this configuration, the upper Delta II stage has been removed from the launch vehicle, and the CM/SM is directly mounted to the first stage using the spacecraft adapter. The CM/SM is fully loaded with propellant for the lunar mission (7909.8 k). As will be demonstrated, a significant portion of this ΔV is used, but sufficient reserve for onorbit maneuvering and deorbit will remain. The SM engine is fired twice: first to raise the orbit apogee to the ISS altitude and then to circularize and trim the final orbit. Figure 16 shows the proposed CONOPS, and the table in Fig. 16 shows the mission timeline from launch to final-orbit insertion. As stated previously, this trajectory is intended only to demonstrate the mission feasibility; phasing orbits required to rendezvous the ISS are not considered in this analysis.

Figure 17 presents the optimized trajectory, showing time-history profiles for altitude, pitch angle, acceleration, and velocity. Here, the target apogee at stage 2 burnout was 350 km, and the resulting

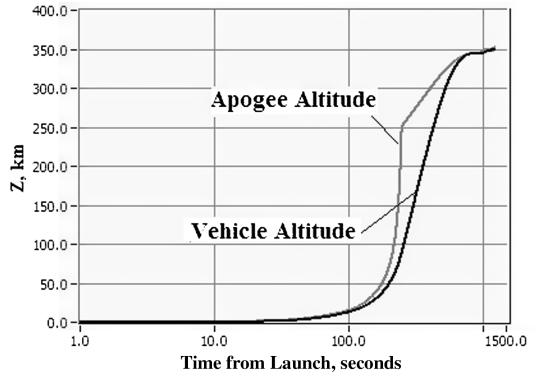

a) Geometric altitude/orbit apogee

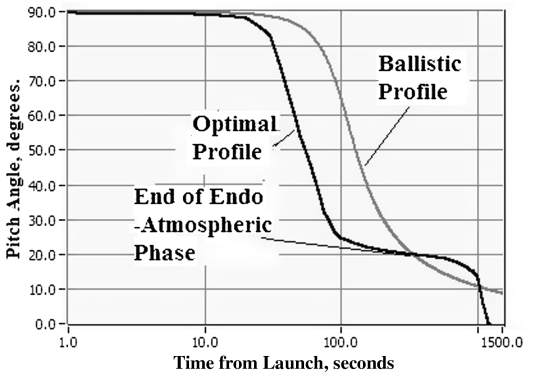

b) Pitch angle

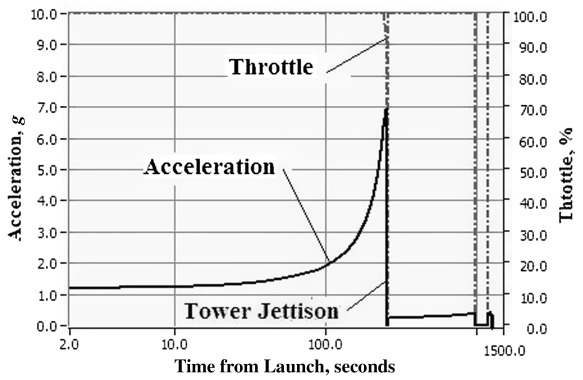

c) Onboard acceleration, throttle

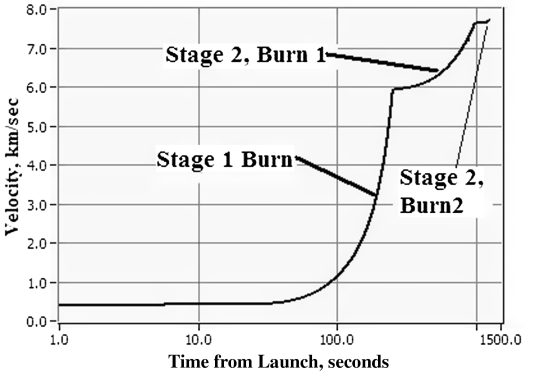

d) Inertial velocity

Fig. 15 Atlas IV HLV CM/SM active optimal trajectory.

optimized parameter pair is $\{\lambda = 0.1006\ \text{s}^{-0.54},\ n = 0.539\}$. For the trajectory, the endoatmospheric optimization routine was terminated at the first stage 2 burn shutoff (989.65 s) and then manually faired to zero for the circularization and trim burn. Here, the longer burn time for the first stage is due to more downthrottling required to keep the acceleration loads under 7.0*g*. The very long duration Keplerian coast period results from the low thrust of the CV/SM AJ-10 engine when compared with the baseline upper stage's RL10B-2 engine. When the optimizer finally places the orbit apogee at 350 km altitude, the orbit is already very nearly circular, and the spacecraft is only slightly past apogee. Thus, almost a complete orbit is required before the final trim burn can be efficiently performed.

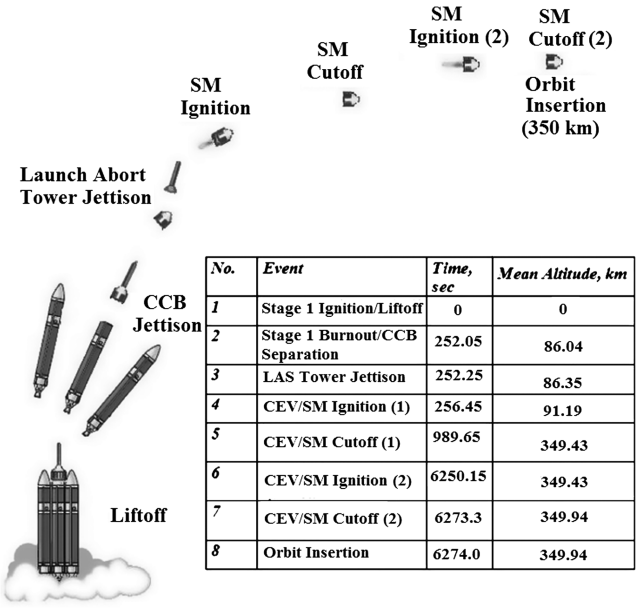

No.	Event	Time, sec	Mean Altitude, km
1	Stage 1 Ignition/Liftoff	0	0
2	Stage 1 Burnout/CCB Separation	252.05	86.04
3	LAS Tower Jettison	252.25	86.35
4	CEV/SM Ignition (1)	256.45	91.19
5	CEV/SM Cutoff (1)	989.65	349.43
6	CEV/SM Ignition (2)	6250.15	349.43
7	CEV/SM Cutoff (2)	6273.3	349.94
8	Orbit Insertion	6274.0	349.94

Fig. 16 Delta IV three-CCB CM/SM active CONOPS.

For the two burns, the CM/SM consumes 7305.22 kg of propellant, with only 604.48 kg of propellant remaining after the final trim burn. Allowing for the 505.48 kg of propellant required for deorbit and reentry, the margin remaining for orbital maneuvering is now down to 99.0 kg. This margin is slim, but it is probably acceptable, because the reaction control maneuvering propellant is assumed to have full capacity at this point.

D. Simulation Data Summary

Table 6 summarizes the results of the simulation studies for the launch configurations shown in Fig. 10. The key here is the residual onorbit ΔV for the Orion spacecraft. It must be noted that the final-orbit eccentricity is an artifact of the simulation resolution. Higher-fidelity simulations with significantly lower sample intervals will result in very precise final-orbit insertions. Because this study was intended only to demonstrate the feasibility of the proposed configurations, this final-orbit imprecision is not a concern. The gross takeoff mass (GTOM) includes the estimated weights of interstage adapters [21] and the LAS system. Of interest here is the residual onorbit ΔV that is available to the CM/SM for maneuvering and deorbit. All three configurations maintain some reserve, with configuration 2 being the most desirable with regard to this ΔV performance criterion.

E. First-Stage Impact Assessment

Because of the unconventional configurations and launch trajectories presented in the previous section, it is essential that the impact points of the spent EELV first stages be considered. These results are presented in Figs. 18–20. For this analysis, the simulation discussed in Sec. V was used to predict the first-stage impact trajectory. For this analysis, drag coefficients due to a tumbling booster were not considered. Only the nominal aerodynamic coefficients from Figs. 9 and 10 were used. These aerodynamic coefficients were perturbed by as much as 25% and found to have only a minimal effect on the impact points.

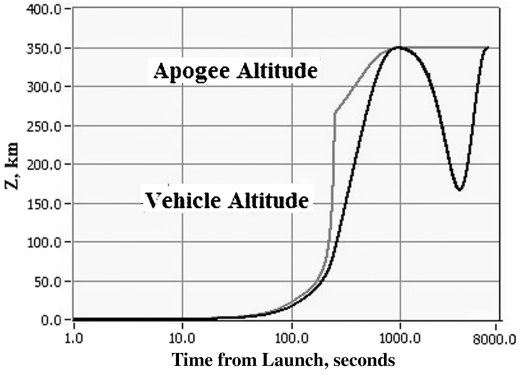

a) Geometric altitude/orbit apogee

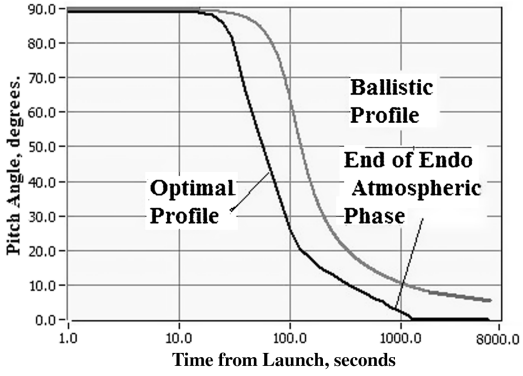

b) Pitch angle

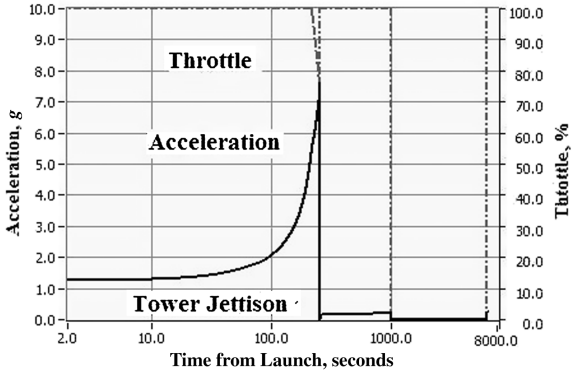

c) Onboard acceleration, throttle

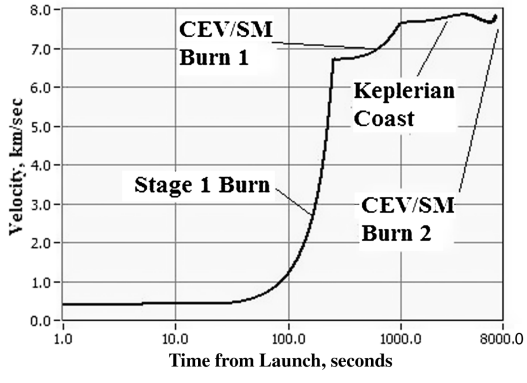

d) Inertial velocity

Fig. 17 Delta IV three-CCB CM/SM active optimal trajectory.

Table 6 Simulation results summary for the three proposed EELV-derived configurations

Configuration	GTOM, kg (lbs)	Stage 1 propellant burned, kg (lbs)	Stage 2 propellant burned, kg (lbs)	CM/SM propellant burned, kg (lbs)	Onorbit residual ΔV m/s (ft/s)	e_{final}	Z_{final} km (nm)
1) Atlas V HLV	883,041	773,100	20,830	2825.6	172.6	0.0004	349.94
CM/SM active	(1,836,022)	(1,703,912)	(45,909)	(6277.6)	(566.3)		(188.87)
2) Delta IV heavy	741,959	598,800	25,260	0	692.1	0.00017	350.02
CM/SM passive	(1,635,278)	(1,319,755)	(55,673)	(0)	(2270.6)		(188.91)
3) Delta IV, 3-CCB	710,989	598,800	——	7305.3	125.2	0.00027	349.94
CM/SM active	(1,567,029)	(1,319,755)	(——)	(16,100.9)	(410.6)		(188.87)

Figure 18 plots the first-stage trajectories and impact points for the Atlas V HLV CM/SM active configuration. Figure 18a plots the first-stage altitude versus downrange for four different trajectories: 1) an ascending node launch with no first-stage throttling, 2) an ascending node trajectory with first-stage throttling required to keep the launch gravity loads below 7.0, 3) a descending node trajectory with no first-stage throttling, and 4) a descending node trajectory with first-stage throttling required to keep the launch gravity loads below 7.0. Figure 18b plots the predicted first-stage ground tracks and impact points. The predicted ascending node impact points are in the Atlantic Ocean, well short of the European continent. Because of the heavy mass of the upper stage, throttling is necessary only right before stage 1 burnout, and it has only a small effect on the impact-point location. Descending-node first-stage impacts are deep within the Amazon basin. These impact points preclude descending-node launches for this Orion/EELV configuration.

Figure 19 plots the first-stage trajectories and impact points for the Delta IV heavy CM/SM passive configuration. Figure 19a plots the first-stage altitude versus downrange for four different trajectories: 1) an ascending-node launch with no first-stage throttling, 2) an ascending-node trajectory with first-stage throttling, 3) a descending-node trajectory with no first-stage throttling, and 4) a descending-node trajectory with first-stage throttling. Figure 18b plots the predicted first-stage ground tracks and impact points. The first-stage trajectories and impact points are very similar to the previous Atlas V trajectories. The predicted ascending-node impact points are in the Atlantic Ocean, well short of the European continent. Descending-node first-stage impacts are within the Amazon basin and preclude descending-node launches for this Orion/EELV configuration.

Figure 20 plots the first-stage trajectories and impact points for the Delta IV 3 × CCB CM/SM Active configuration. Figure 20a plots the first-stage altitude versus downrange for four different trajectories: 1) an ascending-node launch with no first-stage throttling, 2) an ascending-node trajectory with first-stage throttling, 3) a descending-node trajectory with no first-stage throttling, and 4) a descending-node trajectory with first-stage throttling. The first-stage trajectories and impact points are significantly different than the trajectories presented in Figs. 18 and 19.

For the Delta IV option without the upper stage, because of the relatively low launch mass, throttling occurs over a significantly longer time period and has a significant effect on the upper-stage trajectory and impact point. This impact point is in contrast to the unthrottled profile, which places the upper-stage impact point in central Europe. This throttling has the fortunate effect of shortening the impact point well short of the European continent. Descending-node first-stage impacts are within the Amazon basin, or uncomfortably close to the Brazilian mainland. These impact points preclude descending-node launches for the Orion/EELV configurations.

With all three of the descending-node trajectories, presented in Figs. 18–20, it may be possible to stretch the trajectory to place the first-stage impact point well off of the Brazilian coast; however, these options were not addressed in this feasibility analysis. Fortunately, there exists a launch option for each configuration that places the impact point of the expended first stage comfortably offshore in the Atlantic Ocean.

VII. Reliability Assessment

A full reliability assessment for the three proposed configurations is beyond the scope of this analysis; however, complete reliability figures, developed by Maggio and Hall [51] at the Information Systems Laboratory (ISL) for multiple Delta IV EELV configurations, are summarized and presented here. Fortunately, configuration 2 (Delta IV heavy CM/SM passive) and configuration 3 (Delta IV 3-CCB CM/SM active) were permutations directly assessed by this team. The Delta IV reliability data will be extrapolated to give risk assessments for the Atlas V configuration (Atlas V HLV CM/SM active). Loss-of-mission (LOM) reliability assessments for the launch vehicle configurations will be presented first. These estimates will be followed by loss-of-crew (LOC) estimates that factor in reliability numbers for the Orion LAS.

A. Loss of Mission Assessments

Tables 7 and 8 summarize the reliability assessment for the Delta IV heavy CM/SM passive configuration. The presented numbers represent probabilities of critical failures that result in

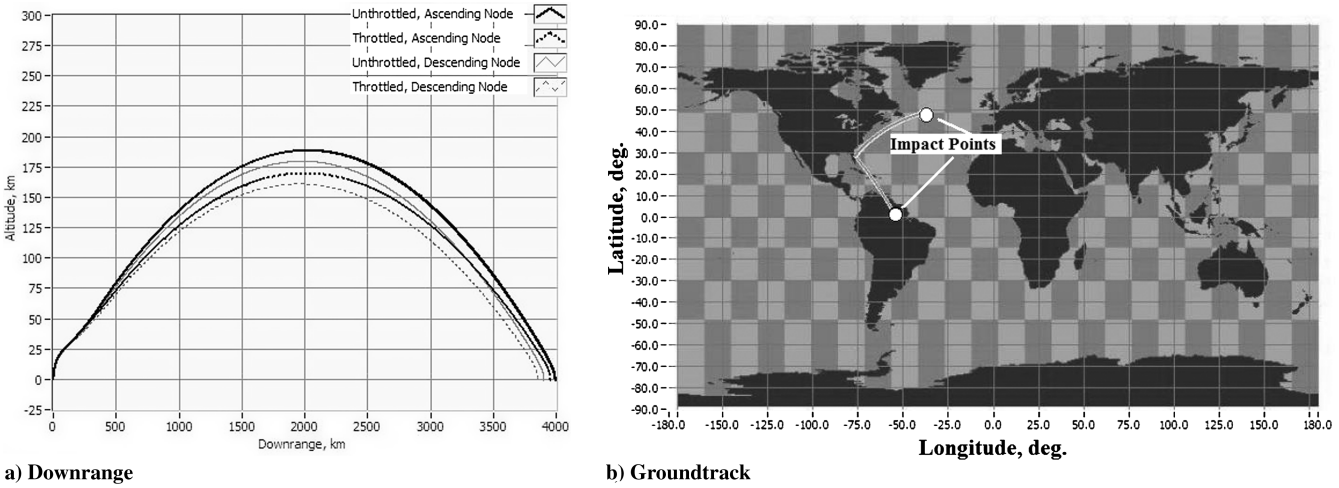

a) Downrange b) Groundtrack

Fig. 18 Atlas V HLV CM/SM active first-stage downrange, ground track, and impact points.

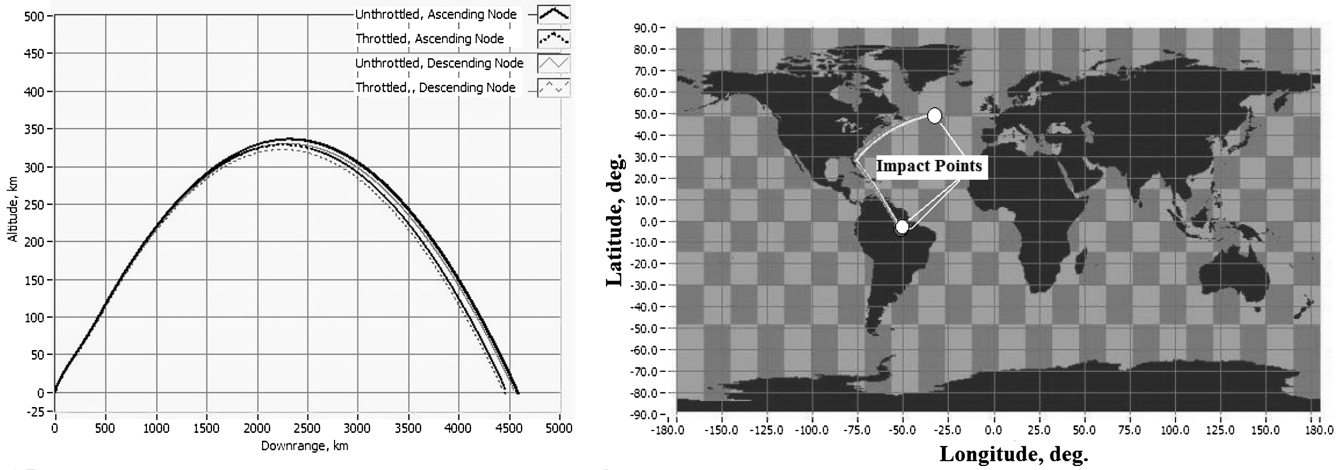

a) Downrange b) Groundtrack

Fig. 19 Delta IV heavy CM/SM passive, first-stage downrange, ground track, and impact points.

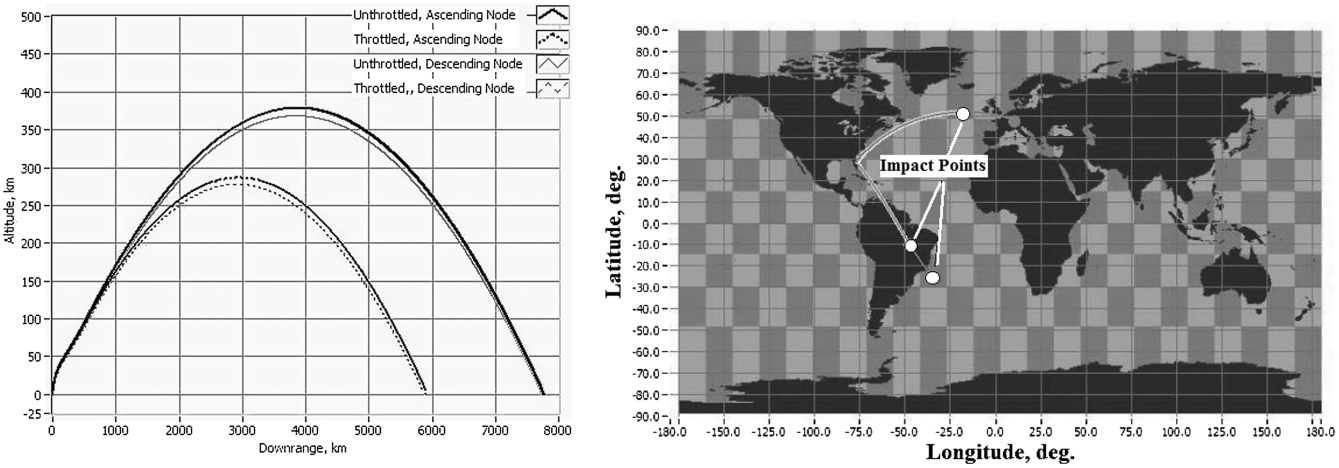

a) Downrange b) Groundtrack

Fig. 20 Delta IV three-CCB CM/SM active first-stage downrange, ground track, and impact points.

LOM. Stage 1 CCB startup failures are not considered. It is assumed that if one of the three CCBs fails to ignite, the mission will be aborted, and the stages will be shut down. The other contingency category includes failures of items, like auxiliary power systems, thrust vectoring, throttle control, main power systems, and stage separation. Because the Orion is assumed to be carried as a passive payload, the scope of this risk assessment is from main booster ignition until the final shutoff of the upper- stage engine. The Table 7 assessment considers the reliabilities of the baseline nonhuman-rated EELV configuration. Table 8 presents reliability numbers for the same configuration, except now the components have been human rated. The component reliability numbers are taken directly from Maggio and Hall [51]. Surprisingly, human rating the components only decreases the LOM probabilities from 1/102 to 1/169, a 40% reduction in mission risk.

Tables 9 and 10 summarize the reliability assessment for the Delta IV 3-CCB CM/SM active configuration. Here, the upper-stage failure path has been eliminated from consideration, and the CM/SM propulsion-system failure probabilities are inserted instead. Maggio and Hall [51] only considered this option for human-rated components, but an additional table using baseline EELV values has been added here for completeness. Even though the CM/SM is considered to be extremely reliable, due to its simple hypergolic ignition system design, because the CM/SM is now an active propulsion component, the failure probability must be included in the calculation. The reliability of this modified configuration is only marginally better than the baseline Delta IV heavy with passive payload. However, the total system for the reliability human-rated configuration is significantly greater. The LOM probability has now been reduced by approximately twice that of the baseline EELV configuration and approximately 16% of the human-rated Delta IV heavy passive Orion option.

Tables 11 and 12 present similar calculations for the Atlas V HLV CM/SM active configuration with baseline EELV and human-rated components. The assumed individual component reliabilities are identical to the values in Tables 7–10. Because the CM/SM is required to perform only one burn for this configuration, its engine-startup-failure probability has been reduced by a factor of two. As expected, because there are more active components to be considered, the Atlas V configurations have lower calculated reliability values than the Delta IV-based configurations.

B. Launch-Abort-System Reliability Assessment

It must be recognized that LOM does not necessarily imply LOC. The reliability of the LAS must be factored in for the LOC calculation. Once again, LAS reliability values established by Maggio and Hall [51] will be summarized and presented here. These LAS reliability numbers will be combined with the LOM estimates, presented in Tables 7–12, to establish end-to-end LOC probability assessments. The ISL study used the dynamic abort risk evaluator (DARE) model to perform this assessment. DARE calculates the potential blast yield at the time of booster failure and then determines the critical distance at which the blast pressure wave will no longer cause a critical Orion failure. If Orion (after abort) is outside of the critical region, then a successful abort is assumed to have occurred.

Table 7 LOM reliability assessment for Delta IV heavy CM/SM passive baseline EELV components

Component	Engine startup failure	Contained engine failure	Uncontained engine failure	Other contingency	Component total
Core booster	——	1 in 775	1 in 1204	1 in 357	1 in 357
Strap CCB	——	1 in 430	1 in 711	1 in 222	1 in 222
Delta II (RL-10 B-2 engine) upper stage	1 in 1406 (2 burns)	1 in 1406	1 in 3170	1 in 1977	1 in 399
Vehicle total	——	——	——	——	1 in 102

Table 8 LOM reliability assessment for Delta IV heavy CM/SM passive human-rated components

Component	Engine startup failure	Contained engine failure	Uncontained engine failure	Other contingency	Component total
Core booster	——	1 in 1293	1 in 2040	1 in 2668	1 in 610
Strap CCB	——	1 in 656	1 in 1093	1 in 2352	1 in 349
Delta II (RL-10 B engine) upper stage	1 in 2564 (2 burns)	1 in 1815	1 in 5593	1 in 3558	1 in 714
Vehicle total	——	——	——	——	1 in 169

Conservatively, the numbers to be presented here assume a 100% probability that a stage 1 failure will propagate to stage 2 and cause a failure there also. The blast center was assumed to be distributed uniformly over the length of the first stage.

The abort effectiveness varies only slightly amongst the configuration studies by Maggio and Hall [51], and the mean crew-abort effectiveness (CAE) index was established at 0.83. That is, 83% of the abort missions will be survived by the crew with minimal injury to all members. Combining the CAE value with the LOM numbers gives a rough assessment of LOC numbers. Table 13 summarizes the LOM and LOC assessments for all the configuration permutations presented in this paper. Conservatively, for this analysis, it is assumed that the LAS is jettisoned after stage 1 burnout and is not available for crew egress after that point. Clearly, extending the tower jettison altitude to cover the first of the stage 2 ignitions and burns would decrease the LOC probability.

The numbers presented in Table 13, even for the nonhuman-rated components, are consistently better than the actual space shuttle operational numbers. As of the date of this publication, the space shuttle program has lost two missions, with the vehicles destroyed and crew lost, in 131 total missions. This statistic translates to LOM and LOC probabilities of 1 in 65.5. In total, the U.S. has launched 158 crewed space missions, with the additional LOM on Apollo 13 (the crew survived). The complete operational reliability LOM statistics for all U.S. human spaceflight efforts is 1 in 52.7. The U.S. space LOC probability is 1 in 79. The official NASA LOC value for the space shuttle program is 1 in 423. It must be noted that the LOC values presented in Table 13 are lower than the stated NASA LOC value of 1 in 1918 for the Ares I/Orion configuration [52]. It is unclear how NASA established this assessment.

VIII. Development Costs

If the LOC values for the Ares I, as stated by NASA, are accurate, then data presented in Table 13 show that the baseline EELV-derived configurations are not competitive in terms of crew safety. However, if the components are human rated, then a good case for comparative crew safety can be established. Because of the Orion/Ares I configuration uncertainty, it is difficult to make a one-to-one development cost comparison between the human-rated EELVs and the Ares I. Florida Today performed such a comparison in early 2009 and published the data on 08 February 2009 [53]. Florida Today's data are summarized in Table 14. NASA's stated cost per flight for Ares I is significantly lower than for both EELVs; however, the U.S. Department of Defense has expended more than $20 billion on the EELV development, and this investment has resulted in a production, assembly, and launch infrastructure that has yet to be developed for the Ares I. When nonrecurrent engineering cost investments are included, the Ares I cost per flight could rise dramatically before the system becomes operational, making the EELVs more than cost competitive. Because the EELVs are already operational, and the launch procedures and infrastructure are well established, it stands to reason that adapting EELVs for the Orion flights offers the potential

Table 9 LOM reliability assessment for Delta IV Three-CCB CM/SM active baseline EELV components

Component	Engine startup failure	Contained engine failure	Uncontained engine failure	Other contingency	Component total
Core booster	——	1 in 775	1 in 1204	1 in 357	1 in 357
Strap CCB	——	1 in 430	1 in 711	1 in 222	1 in 222
Orion SM	1 in 2726 (2 burns)	1 in 51,800	1 in 54,923	1 in 12,419	1 in 2063
Vehicle total	——	——	——	——	1 in 128

Table 10 LOM reliability assessment for Delta IV three-CCB CM/SM active human-rated components

Component	Engine startup failure	Contained engine failure	Uncontained engine failure	Other contingency	Component total
Core booster	——	1 in 1293	1 in 2040	1 in 2668	1 in 610
Strap CCB	——	1 in 656	1 in 1093	1 in 2352	1 in 349
Orion SM	1 in 2726 (2 burns)	1 in 51,800	1 in 54,923	1 in 12,419	1 in 2063
Vehicle total	——	——	——	——	1 in 200

Table 11 LOM reliability assessment for Atlas V HLV CM/SM active baseline EELV components

Component	Engine startup failure	Contained engine failure	Uncontained engine failure	Other contingency	Component total
Core booster	——	1 in 775	1 in 1204	1 in 357	1 in 357
Strap CCB	——	1 in 430	1 in 711	1 in 222	1 in 222
Centaur III (RL10A-4-2 engine) upper stage	1 in 1406 (2 burns)	1 in 1406	1 in 3170	1 in 1977	1 in 399
Orion SM	1 in 5452 (1 burn)	1 in 51,800	1 in 54,923	1 in 12,419	1 in 3317
Vehicle total	——	——	——	——	1 in 99

Table 12 LOM reliability assessment for Atlas V HLV CM/SM active human-rated components

Component	Engine startup failure	Contained engine failure	Uncontained engine failure	Other contingency	Component total
Core booster	——	1 in 1293	1 in 2040	1 in 2668	1 in 610
Strap CCB	——	1 in 656	1 in 1093	1 in 2352	1 in 349
Centaur III (RL10A-4-2 engine) upper stage	1 in 2564 (2 burns)	1 in 1815	1 in 5593	1 in 3558	1 in 714
Orion SM	1 in 5452 (1 burn)	1 in 51,800	1 in 54,923	1 in 12,419	1 in 3317
Vehicle total	——	——	——	——	1 in 161

for a considerably compressed schedule when compared to the Ares I development.

IX. Conclusions

With the space shuttle set to retire in early 2011, it is important that the Ares I become operational as soon as possible. During this interim period, NASA must rely on the Russian Soyuz or, possibly, COTS for crew access to the station. Even if this timeline is 100% successfully achieved, there will exist a 5 year operations gap in which the U.S. will not have self-determined access to the ISS. Any further delay in the Ares I schedule will significantly impact, and could terminate, the ISS science and mission operations. This paper explores interim mission scenarios. using existing EELVs for delivering Orion to the ISS. The use of existing COTS is proposed to narrow the ISS service gap from the time the space shuttle is deserviced until the Ares I is crew rated and operational.

Three launch options are evaluated: 1) Atlas V HLV, 2) Delta IV heavy, and 3) Delta IV with three CCBs as a first stage, with Orion acting as the second stage. Configurations 1 and 3 require significant impulse from the Orion's SM engine to achieve the final orbit. Configuration 2 launches Orion as a passive payload without reliance on any impulse from the SM. All three configurations reserve sufficient SM impulse for deorbit and reentry. Extensive simulation studies were performed to demonstrate mission feasibility for the three proposed configurations. The simulations were developed using data gathered from a variety of public-domain sources. These sources were cross referenced for accuracy. An equilibrium gas-chemistry code was used to model the combustion products, based on mean properties for the specified propellants. As required, thermochemical data were adjusted to give consistency between the specified engine performance and the propulsive stage models. Launch configuration aerodynamics were evaluated using an industry-standard analytical aerodynamics code. The simulation studies demonstrate that all three of the proposed configurations reach the ISS orbit with sufficient propellant margin to allow for deorbit and reentry.

Table 13 LOM/LOC summary for three proposed EELV-derived configurations (83% CAE)

Configuration	Baseline EELV components LOM (LOC)	Human-rated components LOM (LOC)
1) Atlas V HLV, CM/SM active	1 in 99 (1 in 247)	1 in 161 (1 in 405)
2) Delta IV heavy CM/SM passive	1 in 102 (1 in 267)	1 in 169 (1 in 461)
3) Delta IV 3-CCB CM/SM active	1 in 128 (1 in 579)	1 in 200 (1 in 937)

Table 14 Development cost comparisons

Launch platform	Development cost, $ billion	U.S. investment to date, $ billion	Cost per flight, $ million
Ares I	4.6	2	120
Delta IV heavy	3.65	12–16	350
Atlas V HLV	4.2	12–16	350

Reliability estimates derived from public release documents demonstrate that, when the EELV components are human rated, the proposed configurations will be competitive with the NASA-stated Ares I reliability and will have significantly lower LOM/LOC estimates than currently stated by NASA for the space shuttle. This study demonstrates feasibility for accomplishing the ISS crew mission, using only the first stage of the Delta IV heavy and the Orion/SM fully loaded with propellant for the lunar mission. This configuration has the distinct advantage of simplifying the launch stack, thereby reducing potential failure paths. The proposed configuration also eliminates the need to human rate the upper-stage configuration. Because only the CCB needs to be human rated for this configuration, there exists a tremendous potential for schedule compression and cost savings.

The stated cost per flight for the Ares I is significantly lower than for both EELVs; however, the U.S. Department of Defense has expended more than $20 billion on EELV development, and this investment has resulted in a production, assembly, and launch infrastructure that has yet to be developed for the Ares I. When nonrecurrent engineering cost investments are included, the Ares I cost per flight could rise dramatically before the system becomes operational, making the EELVs cost competitive. Because the EELVs are already operational, and the launch procedures and infrastructure are well established, there is a high probability that using these systems will result in a considerably compressed schedule when compared to the Ares I development schedule.

References

[1] Anon., "NASA's Exploration System Architecture Study," NASA TM-2005-214062, Nov. 2005.

[2] "Overview: Ares I Crew Launch Vehicle," NASA, http://www.nasa.gov/mission_pages/constellation/ares/aresl/index.html [retrieved

30 Sept. 2008].
[3] Anon., "Overview: Ares V Cargo Launch Vehicle," NASA, http://www.nasa.gov/mission_pages/constellation/ares/aresV/index.html [retrieved 30 Sept. 2008].
[4] "Space Commerce," U.S. Dept. of Commerce, http://www.space.commerce.gov/transportation [retrieved 20 March 2010].
[5] "NASA to Use Russian Rockets if COTS Fails," *Space Pragmatism* [online journal], http://spacepragmatism.net/2009/05/nasa-to-use-russian-rockets-if-cots-fails.html [retrieved 10 Aug. 2009].
[6] Morring, F. J., "Thrust Oscillation Issue Threatens Ares I Design," *Aviation Week and Space Technology* [online journal], Jan. 2008, http://www.aviationweek.com/aw/generic/story.jsp?id=news/aw012808p2.xml&headline=Thrust Oscillation Issue Threatens Ares I Design&channel=space [retrieved 19 Nov. 2008].
[7] Blomshield, F. S., "Lessons Learned In Solid Rocket Combustion Instability," 43rd AIAA/ASME/SAE/ASEE Joint Propulsion Conference and Exhibit, AIAA Paper 2007-5803, 2007.
[8] Anon., "Crew Safety," *Man-Systems Integration Standards*, NASA STD 3000, Vol. 1, Sec. 6, http://msis.jsc.nasa.gov/sections/section06.htm [retrieved 19 Aug. 2008].
[9] Anon., "NASA and ATK Successfully Test Ares First Stage Development Motor," *Popular Mechanics* [online journal], Sept. 2009, http://www.popularmechanics.co.za/content/news/singlepage.asp?key=846 [retrieved 31 Dec. 2009].
[10] "Ares I-X Flight Test," NASA, http://www.nasa.gov/mission_pages/constellation/ares/flighttests/aresIx/index.html [retrieved 31 Dec. 2009].
[11] Bergin, C., "Pad 39B Suffers Substantial Damage from Ares I-X Launch: Parachute Update," *NASA Spaceflight.com* 31 Oct. 2009, http://www.nasaspaceflight.com/2009/10/pad-39b-suffers-substantial-damage-ares-i-x-parachute-update [retrieved 31 Dec. 2009].
[12] Harwood, W., "NASA Assessing Parachutes and Dented Ares 1-X Booster", *Spaceflight Now*, 29 Oct. 2009, http://www.spaceflightnow.com/ares1x/091029dent [retrieved 31 Dec. 2009].
[13] Augustine, N. R., Austin, W. M., Chyba, C., Kennell, C. F., Bejmuk, B. I., Crawley, E. F., Lyles, L. L., Chiao, L., Greason, J., and Ride, S. K., "Seeking a Human Spaceflight Program Worthy of a Great Nation" [online report], Oct. 2009, http://www.nasa.gov/pdf/396093main_HSF_Cmte_FinalReport.pdf [retrieved 31 Dec. 2009].
[14] Harland, D. M., and Catchpole, J. E., *Creating the International Space Station*, Springer–Praxis, New York, March 2002, pp. 194–198.
[15] Chiulli, R. M., *International Launch Site Guide*, Aerospace Press, El Segundo, CA, 1994, pp. 16–18.
[16] Whitmore, S. A., Bingham, B., and Young, Q., "Deployment of a High-Latitude Dynamic E-Field Pico-Satellite Sensor Constellation," *International Review of Aerospace Engineering*, Vol. 1, No. 4, Aug. 2008, pp. 560–567.
[17] "Evolved Expendable Launch Vehicle," Air Force Space Command, http://www.afspc.af.mil/library/factsheets/factsheet.asp?id=3643 [retrieved 10 Aug. 2009].
[18] Holguin, M. J., "Atlas as a Human-Rated Launch Vehicle," *Proceedings of the Space and Technology Applications International Forum*, 15 Feb. 2006, http://www.highfrontier.org/Archive/hf/STAIF 2006 Atlas Human Rating.pdf [retrieved 20 Dec. 2009].
[19] Pulliam, G., "Initial Summary of Human-Rated IV Heavy Study," Aerospace Corp., El Segundo, CA, 17 June 2009, http://www.nasa.gov/pdf/361063main_20090617AerospaceHSF.pdf [retrieved 20 March 2010].
[20] Anon., "Constellation, Orion Crew Exploration Vehicle," NASA FS-2008-07-031-GRC, http://www.nasa.gov/pdf/306407main_orion_crew%20_expl_vehicle.pdf [retrieved 20 March 2010].
[21] Isakowitz, S. J., Hopkins, J. P., Jr., and Hopkins, J. B., *International Reference Guide to Space Launch Systems*, 4th ed., AIAA, Reston, VA, 2003, Chaps. 4, 6.
[22] Anon., "Delta IV Payload Planners Guide," United Launch Alliance, Littleton, CO, Sept. 2007, http://www.scribd.com/doc/16924978/Boeing-Delta IV-Payload-Planners-Guide [retrieved 20 Dec. 2009].
[23] Boeing Delta IV Launch Video, The Boeing Co., St. Louis, MO, http://www.boeing.com/defense-space/space/delta/d4_webcast.html [retrieved 15 July 2009].
[24] "Delta IV Heavy: First Flight" [online photo gallery], The Boeing Co., St. Louis, MO, http://www.boeing.com/companyoffices/gallery/images/space/delta_iv/delta_iv_1st_heavy1.htm [retrieved 15 July 2009].
[25] "Telecommunications Satellite Launches with Heavy Payload," *FoxNews.com*, 14 April 2008, http://www.foxnews.com/story/0,2933,351292,00.html [retrieved 10 Aug. 2009].
[26] "Atlas V EELV: Lockheed Martin," Global Security, http://www.globalsecurity.org/space/systems/atlas-v.htm [retrieved 20 March 2010].
[27] Anon., "Atlas Launch System Mission Planner's Guide, Revision 10a," Lockheed–Martin Rept. CSLB-0409-1109, Jan. 2007, http://www.lockheedmartin.com/data/assets/ssc/Rev10a_0107.pdf [retrieved 22 Dec. 2009].
[28] "Atlas V," United Launch Alliance Houston, TX, http://www.ulalaunch.com/docs/product_sheet/AtlasProductCardFinal.pdf [retrieved 10 Aug. 2009].
[29] Brauer, G. L., Cornick, D. E., and Stevenson, R., "Capabilities and Applications of the Program to Optimize Simulated Trajectories (POST), Program Summary Document," NASA CR-2770, Feb. 1977.
[30] Evans, M. B., and Schilling, L. J., "The Role of Simulation in the Development and Flight Test of the HIMAT Vehicle," NASA TM-84912, Edwards, CA, April 1984.
[31] Sobol Ilya, M., *A Primer for the Monte Carlo Method*, CRC Press, Boca Raton, FL, 1994, Chaps. 1–3.
[32] Vallado, D. A., *Fundamentals of Astrodynamics and Applications*, 2nd ed., Microcosm, Hawthorne, CA, 2001, Chap. 4.
[33] Haering, E. A., Jr., and Whitmore, S. A., "FORTRAN Program for the Analysis of Ground Based Range Tracking Data: Usage and Derivations," NASA TM 104201, 1992.
[34] Anon., "United States Standard Atmosphere, 1976," National Oceanic and Atmospheric Administration Rept. NOAA-S/T-76-1562, Washington, D.C, 1976.
[35] Justus, C., G. (ed.), "Earth Global Reference Atmosphere Model (GRAM-2007)", NASA Space Environments and Effects Program, http://see.msfc.nasa.gov/tte/model_gram.htm [retrieved 20 March 2010].
[36] Anderson, J. D., *Modern Compressible Flow with Historical Perspectives*, 3rd ed., McGraw–Hill, New York, 2003, Chap. 3.
[37] Sutton, G. P., and Biblarz, O., *Rocket Propulsion Elements*, 7th ed., Wiley, New York, 2001, Chap. 3.
[38] Gordon, S., and McBride, B. J., "Computer Program for Calculation of Complex Chemical Equilibrium Compositions and Applications," NASA RP-1311, 1994.
[39] Zeleznik, F. J., and Gordon, S., "Calculation of Complex Chemical Equilibria," *Journal of Industrial and Engineering Chemistry*, Vol. 60, No. 6, 1968, pp. 27–57. doi:10.1021/ie50702a006
[40] Milstead, A. H., "Deboost from Circular Orbits," *Journal of the Aeronautical Sciences*, Vol. 13, No. 4, July–Aug. 1966, pp. 170–171.
[41] Vukelich, S. R., Stoy, S. S., Burns, K. A., Castillo, J. A., and More, M. E., "Missile DATCOM Volume 1: Final Report," Air Force Wright Aeronautical Labs., TR-86-3091, 1988.
[42] Sooy, T. J., and Schmidt, R. Z., "Aerodynamic Predictions, Comparisons, and Validations Using Missile DATCOM (97) and Aero-Prediction 98 (AP98)," 42nd AIAA Aerospace Sciences Meeting and Exhibit, AIAA Paper 2004-1246, 2004.
[43] Blake, W. B., "Missile DATCOM User's Manual: 1997 FORTRAN 90 Revision," Air Force Wright Aeronautical Labs., VA-WP-TR-1998-3009, Feb. 1998.
[44] Hammond, W., *Design Methodologies for Space Transportation Systems*, AIAA Education Series, AIAA, Washington, D.C., 2001.
[45] Zipfel, P. H., *Modeling and Simulation of Aerospace Vehicle Dynamics*, AIAA Education Series, Reston, VA, 2001, pp. 76–78.
[46] Cobleigh, B. R., "Development of the X-33 Uncertainty Model," NASA TP-1998-206544, April 1998.
[47] Sellers, J. J., *Understand Space: An Introduction to Astronautics*, 5th ed., McGraw–Hill, New York, 2005, Chap. 14.
[48] Rade, L., and Westergren, B., *Beta-Mathematics Handbook*, 2nd ed., CRC Press, Boca Raton, FL, 1990, pp. 331–332.
[49] Whitmore, S. A., and Smith, T., "Launch and Deployment Analysis for a Small, MEO, Technology Demonstration Satellite," *Journal of Spacecraft and Rockets*, Vol. 46, No. 2, March–April 2009, pp. 449–458. doi:10.2514/1.39832
[50] Anon., "Man-Systems Integration Standards, Volume 1—Standards," NASA STD 3000, July 1995, http://msis.jsc.nasa.gov/volume1.htm [retrieved 29 Dec. 2009].
[51] Maggio, G., and Hall, T., "Safety and Reliability Assessment of Delta IV EELV Based Crew Launch Options," Information Systems Labs, San Diego, CA, 10 June 2009, http://images.spaceref.com/news/2009/SRA.EELV.pdf [retrieved 1 Aug. 2009].
[52] Halvorson, T., "Griffin Says Ares I is Two Times Safer," *Florida Today* [online newspaper], 08 Feb. 2009, http://www.floridatoday.com/assets/pdf/A912809629.PDF [retrieved 1 Aug. 2009].
[53] Halvorson, T., "Rocket Analysis: A Look at What Could Sway Obama's Decision on a New Launch Vehicle for NASA," *Florida Today* [online newspaper], 08 Feb. 2009, http://www.floridatoday.com/assets/pdf/A912809629.PDF [retrieved 1 Aug. 2009].

J. Martin
Associate Editor